Technical University of Liberec
Faculty of Textile Engineering

DIPLOMA THESIS

Ashwin Sheolal

Technical University of Liberec

Faculty of Textile Engineering

Department of Textile Technology

Application of air in yarn production using ring-jet and air-jet spinning

Ashwin Sheolal

Supervisor: Professor S. Ibrahim

Consultant : Ing. Petra Jiraskova

Number of pages: 61

Number of figures: 49

Number of tables: 2

Number of appendicies: 1

Statement

I have been informed that my thesis is fully applicable to the Law No. 121/2000Coll. About copyright, especially section §60- school work.

I acknowledge that Technical University of Liberec (TUL) does not breach my copyright when using my thesis for internal need of TUL.

Shall I use my thesis or shall I forward a licence for its utilization, I acknowledge that I am obliged to inform TUL about this. TUL has the right to claim expenses incurred for this thesis up to amount of actual full expenses.

I have elaborated the thesis alone utilising listed literature and on the basis of consultations with the supervisor.

Date: 10th May 2010

Signature: Ashwin Sheolal

Ashwin Sheolal

Acknowledgements

I would first like to thank Professor Sayed Ibrahim for his invaluable inspiration, perseverance and guidance throughout the course of this research. I would like to express my appreciation to Dr. Rajesh Mishra, for his valuable suggestions, comments and assistance in many aspects, from spinning to data analysis. To the laboratory and workshop staff that assisted me with the spinning and tests that were conducted, many thanks. My most sincere gratitude and appreciation goes to Mr. Shamal, for fabricating the required components and instituting the relevant modifications to the machine.

I am deeply grateful to Department of Economic Development of the South African Government for providing funding for my graduate studies. My appreciation goes to the Management of the Durban University of Technology for their enormous support, and granting me the study period. A special thanks to the late Mr. A Budhal, for bestowing a wealth of yarn spinning knowledge, in the foundation years of my career. Last, but not least, I would like to thank my family for their support in my education, and to my friends, who were there for me when I needed them the most.

ABSTRACT

The primary factors influencing the properties and character of staple spun yarns are fiber type and yarn structure. The particular spinning system, each producing yarn of its own distinctive character, determines the yarn structure. The spinning system is in turn dependent upon the manner in which twist is inserted. The recent trend is to use air-jets to insert twist producing yarn of a distinctive, unique structure, consisting of a core and belt or wrapper fibers. Yarn hairiness associated with the longer protruding fibers has been also reduced as a result of this structure. The use of air-jets in the production of yarn therefore has immense potential and is therefore a worthy field of research.

An experimental study using compressed air, delivered by an air-jet, to the fiber stream upon exit from the front roller nip, in an attempt to assemble the fibers into a yarn structure, was conducted. The investigation was divided into the following:

- **Ring-Jet Spinning**

  Consolidating the fibers after drafting using an air-jet by applying false twist to the fibers, and thereafter applying real twist by a spindle on a conventional ringframe.

- **Preliminary investigation into use of air-jets to produce yarn**

  1. An arrangement of two jets in series with two ancillary fiber tubes.

  2. An arrangement of two air-jets in parallel and the third in a series to the first two to produce yarns similar to siro-spun.

For ring-jet spun yarns, the influence on the following yarn parameters was determined, viz. yarn hairiness using Uster and Zwiegle testing equipment, yarn evenness and imperfections determined on Uster and yarn tensile properties on the Instron tester, for the ring- jet yarns.

Key Words

Air-jet, Ring-jet, Air vortex, Spinning, Real twist, False twist, Wrapper fibers, Hairiness

TABLE OF CONTENTS

List of Symbols

C_f	Coefficient of friction	
C_p	Coefficient of friction	
CV%	Coefficient of variation	[%]
d	Diameter	[m]
D	Diameter	[m]
D_r	Draft ratio	
E	Elastic modulus	[Pa]
F	Force	[N]
K	Length	[m]
L	Length	[m]
m_i	Mass	[g]
m_f	Mass flow rate	[Kg/s]
N_s	Rotational speed	[rpm]
p_n	Pressure	[Pa]
T	Twist	[Turns/m]
t	Time	[s]
V_d	Linear speed	[m/min]
X	Elements of regression	
β	Constant of regression	
β_v	Air viscosity – kinematic	[m^2/s]
ρ	Air density	[Kg/m^3]
ρ_f	Fiber density	[Kg/m^3]
τ	Shear stress tensor	[Pa]
μ	Velocity	[m/s]

1. Introduction

It is difficult to precisely specify the time when man first began spinning or converting staple fibers into yarns. There is, however, much archaeological evidence indicating that the skill was practiced at least 8000 years ago. It has been speculated that early man twisted a few fibers of short lengths to form yarn and then tied them together to make longer lengths. With time continuous lengths were produced and this has evolved into a much more sophisticated manner of yarn spinning.

In essence therefore, to convert a staple fiber bundle into yarn, the strength of each fiber in the bundle should be transferred to the other. This is accomplished by twisting the fibers together. The twist, which can either be real or false, dictates the eventual character of the yarn. The method of twist insertion in turn is dependent upon the particular spinning system adopted. Twist increases the frictional forces between fibers and prevents fibers from slipping over one another by generating the radial forces directed towards the yarn interior.

Presently, yam production is a highly advanced technology that involves the engineering of different yam structures having specific properties for particular applications. A detailed understanding of how fiber properties and machine variables are utilised to obtain specific yam structures of appropriate properties is, therefore, an important objective in the study of spinning technology. The current trend is the use of pneumatic techniques in the form of air-jets for the consolidation of the fibers and that will be the basis of the work for the study undertaken.

2 Literature Review

2.1 Principles of Spinning Yarn from Staple Fibers

For staple fibers to be processed or spun into yarn, the following criteria should be satisfied:

- Straightened or linearly orientated fibers.
- Equal number or uniform distribution of fibers along the cross section of the yarn length.
- Tip to end assembly or arrangement of fibers in a "brickwork fashion".
- Consolidation of the fibers by the application of twist, either real of false.
- Winding of the resultant yarn with sufficient and uniform tension.

A definition of yarn spun from staple fibers can thus be formulated as stated below:

A staple-spun yarn is a linear assembly of fibers, held together, usually by the insertion of twist, to form a continuous strand, small in cross section but of any specified length [15]

The determining factor in providing cohesiveness to yarn and imparting the required strength is twist insertion, either real or false. The fibers do however have to be adequately prepared prior to this.

2.2 Real and False Twist

2.2.1 Insertion of Real Twist

Real twist is inserted or applied to a strand of fibers or filaments by holding one end of it fixed (at point A) and rotating it around this axis, either in a clockwise or anti-clockwise direction. This can be extrapolated to the dynamic instance where fibers are held fixed momentarily at the nip point between a set of two rollers (A), and rotated by a revolving spindle (point B). See Figure 1. The amount of twist in a given yarn length can then be quantified as:

$$T = N_s/V_d \qquad (1)$$

Where T = inserted twist (tpm)

N_s = rotational speed of twisting component (rpm)

V_d = delivery rate (m/min)

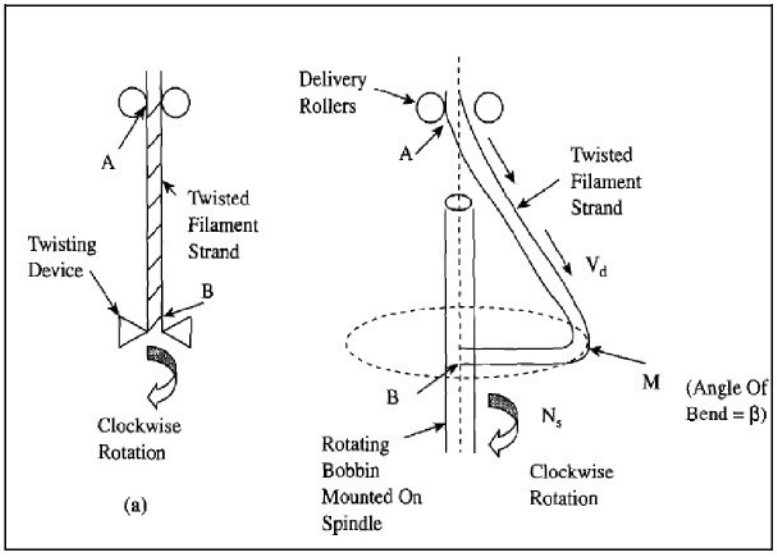

Fig. 1 Real Twist Insertion [15]

2.2.2 False Twisting of Fibers

In the application of false twist, fibers are held or nipped by two pairs of rollers, A and B as shown in Figure 2 whilst being driven at linear speed of V_d m/min. A twist, at the rate of N_s rpm is simultaneously applied at some point X between these two nipping points. The effect is, as shown in the diagram, that the section AX will be rotated clockwise, having 'Z' twist and the section BX rotated counterclockwise, having 'S' twist. The Z-twist in the strand length passing through the AX zone will increase to a constant value of $/V_{d.}$ In zone XB, S-twist will initially be present in the yam length which will increase to a maximum and then decrease to zero. This is because each length of strand moving from zone AX into zone XB will become untwisted by the counterclockwise torque that is present as it enters zone XB.

The time over which the Z-twist builds up to its constant value and the S-twist increases and then decreases to zero may be termed the *transient period.* At the end of this period, the system is said to be in dynamic equilibrium. Z-twist will be observed in the AX zone and no twist will be seen the XB zone. This twisting action is called *false-twisting* since, under dynamic equilibrium, the strand, although being twisted, has no twist when it leaves the twisting device [15].

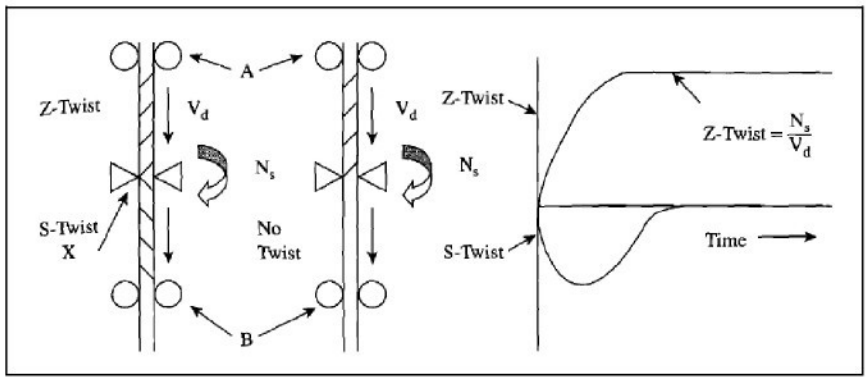

Fig. 2 False Twist Insertion [15]

2.2.3 Derivation of Equation for False twisting

Consider the following segment of yarn:

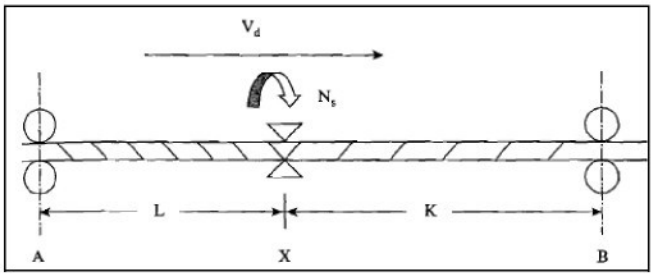

Fig. 3 Section of yarn under false twist

Where N_s = the twist insertion rate in turns per minute

V_d = filament strand speed in mlmin

Zone AX = *L* meters

Zone XB = *K* metres

L does not =*K*

Assumptions:

- At time *t* =0, no twist is present in the strand.
- When twist is inserted in each zone, it is uniformly distributed.
- Twist contraction is negligible.
- At time $t = t_1$, there are *x* turns/m in zone AX, and *y* turns/m in zone XB.

Twlst equation for zone $L = AX$

At time $t = t_1 + dt$ the number of turns in zone AX will be the sum of the following:

- The turns already present =xL.
- The turns inserted by the twisting device = $N_s dt$.
- The turns lost because of the fiber length moving into zone $XB = xV_d dt$.

Thus the twist level in section L at t = $t_1 + dt$ is:

$$T = x + (N_S - xV_d)\,dt/L \quad (1)$$

The change in twist, *dx*, is

$$dx = (N_S - x\,V_d)\,dt/L \quad (2)$$

Rearranging,

$$\int \frac{dx}{N_s - x\,V_d} = \frac{1}{L}\int dt \quad (3)$$

When $t = 0$, $x = 0$, the integral resolves to:

$$x = \frac{N_s}{V_d}\left(1 - e^{-V_d\frac{t}{L}}\right) \quad (4)$$

The twist equation for zone $K = XB$ follows similar reasoning, the change in twist here is given by:

$$dy = \frac{[xV_d - (N_s + V_c\,y)]dt}{K} = -\frac{1}{K}\left[Ne^{-V_d\frac{t}{L}} + V_d\,y\right]dt \quad (5)$$

Rearranging,

$$\frac{dy}{dx} + \frac{V_d\,y}{K} = -\frac{N_s}{K}e^{-V_d\frac{t}{L}} \quad (6)$$

Multiplying throughout by $e^{-V_d\frac{t}{L}}$ and integrating yields:

$$y = -\frac{N_s L}{V_d[L-K]}\left(e^{-V_d\frac{t}{L}} - e^{-V_d\frac{t}{K}}\right) \quad (7)$$

If $L = K$, then

$$y = -\frac{N_s}{K}\left(te^{-V_d\frac{t}{K}}\right) \quad (8)$$

2.3 Twist Insertion in Ring Spun, Rotor Spun and Jet Yarns

Since twist is the major determining factor in the characteristics and performance of staple spun yarns, the manner in which twist is inserted is important and is really dictated by the spinning system utliised. With ring spun yarns, since the spindle is responsible for the creation of twist as well us winding up of the yarn, twist insertion occurs under tension, resulting in a relatively uniform spiraling of the fibers around each other in the yarn structure. An inherent deficiency associated with ring spun yarns however is yarn hairiness, which are the longer protruding fibers from the yarn body. This level of hairiness has been significantly reduced using compact spinning techniques.

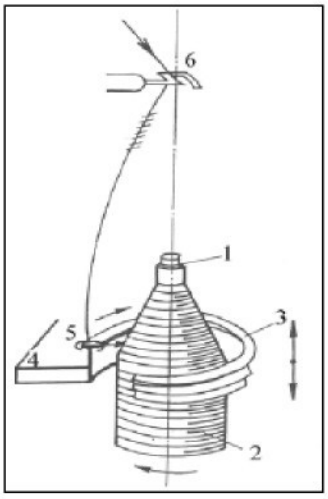

Fig. 4 Twist insertion in ring spinning

In rotor spinning, yarn forms by a rolling action of the fibers in the rotor groove. This rolling action together with the high centrifugal forces generated by the rotating rotor, yields a structure that has a certain degree of intermingling of fibers , with wrapper or binder fibers around the yarn periphery. To insert twist into the fiber ribbon to produce the yarn, sufficient twist torque must be present at point P in Figure 5. This keeps the forming yarn from breaking at P as a result of the high tension induced in AP by centrifugal forces.

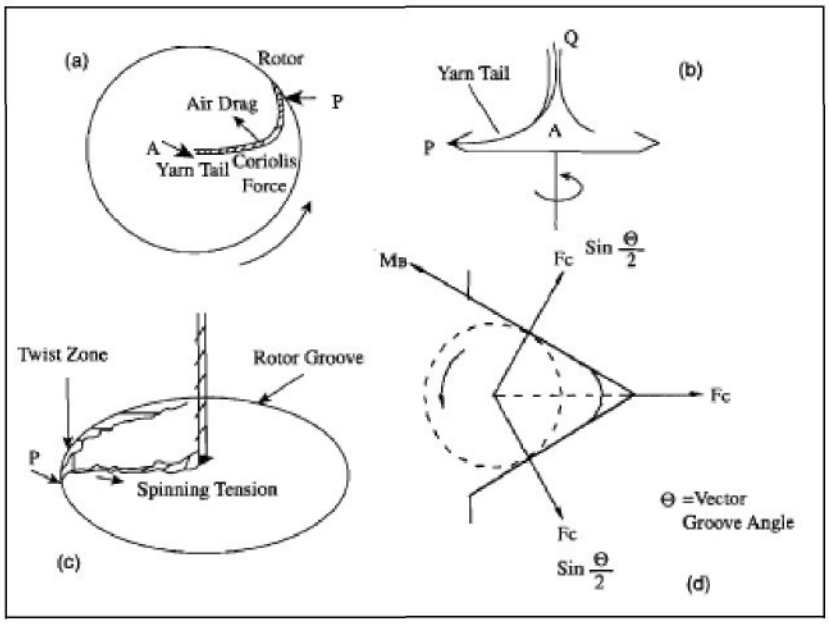

Fig. 5 Twist insertion in rotor spinning

The rotor generates the twist torque as it carries the yarn tail AP through each revolution; QAP is, therefore, similar to a crank. The cranking action induces twist in the length QA. The twist torque builds up and propagates to P. In doing so, it has to overcome the barrier, at A, of the doffing tube and that is caused by the narrowness of the rotor groove.. The spinning tension and the doffing tube geometry are therefore important factors.

Fig. 6 Ring and rotor yarns

In the case of conventional air-jet spinning, the first nozzle which provides airflow in the opposite direction with a weaker intensity than the second nozzle does not affect the core fibers but prevents the edge fibers in the spinning triangle from being twisted in, or twists them in the opposite direction around the core fibers.

The second nozzle imparts a false twist to the fiber bundle that travels back to the front rollers of the drafting unit. Therefore, only the core part, which is the main part of the fiber bundle, is influenced by the second nozzle. Edge fibers either do not have twist or have little twist. When the fiber strand departs the second nozzle, core fibers no longer exhibit any twist. They are arranged in partially parallel form with wrapper fibers around the periphery of the yarn. The fibers do have a certain open-end character, but due to the higher bulk, are softer.

In the case of air vortex spinning, fibers are smoothly sucked into a hollow spindle and twist insertion starts as the fiber bundle receives the force of the compressed air at the inlet of the spindle. The twisting motion tends to propagate from the spindle toward the front rollers. This propagation is prevented by the guide member that temporarily plays a role in the center fiber bundle. After fibers have left the guide member, the whirling force of the air jet separates fibers from the bundle. Since the leading ends of all fibers are moved forward around the guide member and drawn into the spindle by the preceding portion of fiber bundle being formed into a yarn. The air stream in conjunction with the hollow spindle, creates wrapper fibers in a three dimensional manner and the yarn structure borders on rotor and ring spun yarns. Air-jet and air votex spinning is discussed in further detail in sections 2.5.3 and 2.5.4 respectively.

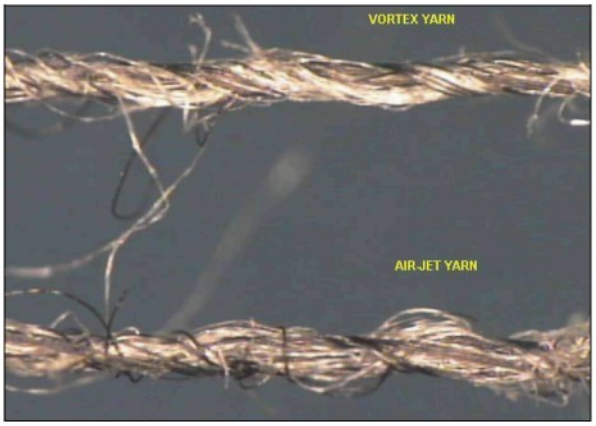

Fig. 7 Vortex and air-jet spun yarns

2.4 Compact Ring Spinning

It can be stated that, despite the low productivity of the ring spinning frame, due to ring-traveler and traveler-yarn friction, it cannot be entirely dispensed with. This is because of the unique character of ring spun yarns that is exceptional for apparel use as well as other diversified applications. It is for this reason that from the 1970's onwards much research work has been devoted to improve the quality and productivity of yarns spun on this system.

One of the major deficiencies associated with ring spun yarns is that of yarn hairiness, which is fiber ends protruding from the yarn body or the main fiber stream, particularly those at the edge. Not only do they adversely affect the yarns performance during subsequent processing, and is the cause of fly liberation, but they also affect the resultant yarn quality. Since these fibers protrude from the main fiber stream, they are not incorporated within it and therefore the number of fibers within the yarn body is less. This results in the strength of the yarn to be slightly less than expected. The fibers are also not well assembled within the yarn body and therefore result in higher unevenness and imperfections. This led to the inception of compact spinning to compensate for these deficiencies.

This modification, to the classical or conventional ring spinning was initialized or conceived by Dr. Ernst Fehrer in 1995 in Switzerland together with Rieter. His work was initially with sliver and was impractical due to the space constraints. Closer examination of his work revealed that the superior yarn quality was a result of the condensation or compacting of the fibers. Pneumatic methods were then incorporated into conventional ringframes to achieve this. Presently this has been adopted by various manufacturers. As the term implies, the fibers that emerge from the nipping zone of the front roller are compacted, thereby reducing the size of the spinning triangle, prior to twist insertion [14].

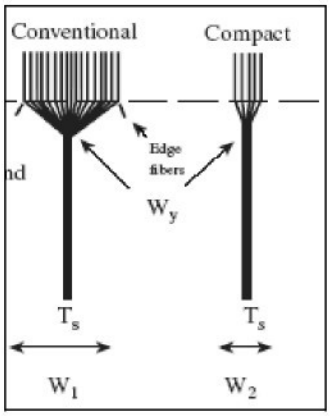

Fig. 8 Spinning triangles of conventional and compact yarns

A control in the dimensions or reduction in the size of the spinning triangle has the following positive impact on yarn quality and characteristics:

- Lower hairiness values.
- Higher strength.
- Improved yarn evenness.
- Less fly liberation during spinning and subsequent processing.
- Improved subsequent processing.

Attempts have therefore been made to reduce the size or to control the dimensions of this spinning triangle. Ringframes with the classical or conventional three-over-three roller and apron drafting system have therefore, incorporated, after the nipping point of the front roller, a compacting mechanism to consolidate or compact the fibers in order to reduce the size of this spinning triangle. The basic principle is illustrated in the Figure 9 below.

1 - Drafing arrangement

1a - Condensing element

1b - Perforated apron

V_z - Condensing zone

2 - Yarn Balloon

3 – Traveler

4 – Ring

5 - Spindle

6 - Ring carriage

7 – Cop

8 - Balloon limiter

9 - Yarn guide

10 – Roving

E - Spinning triangle

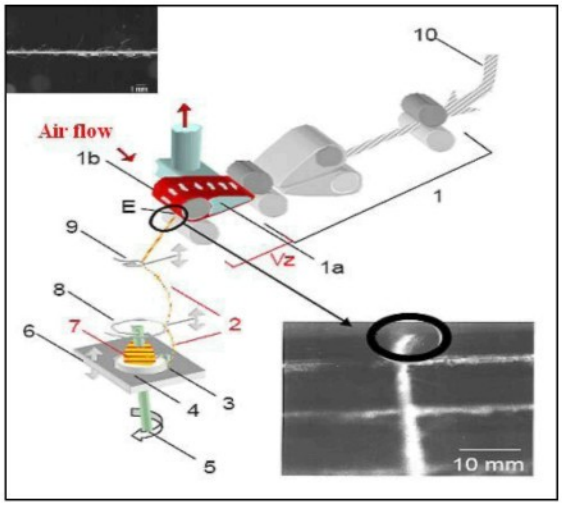

Fig. 9 Principle of compact spinning

Rieter has a system that consists of a perforated drum that is situated just after the double apron arrangement and operates simultaneously as a delivery roller of the system as well as a compacting mechanism. The fiber compacting or consolidation occurs through the suction zone, which is located inside of the perforated roller, and the region between the two pressure rollers [24].

The Sussen compact system consists of a tubular profile, subjected to a negative pressure and a closely embraced lattice apron. The tubular profile has a small slot in the direction of the fiber flow, which commences at the immediate vicinity of the front roll nipping line. This creates an air current through the lattice apron towards the inside of the profiled tube. The air current has a suction effect on the fibers after they leave the front roller nipping line and condenses the fiber strand, which is conveyed by the lattice apron over a curved path to the delivery nipping line. As the slot, being under negative pressure,

reaches right up to the delivery nipping line, the fiber assembly remains totally compacted. This results in a substantial reduction in the dimensions of the spinning triangle. [25]

The Zinser compacting system, is characterised by extending the drafting system by using a double roller. A perforated apron is moved over the upper roller, where the suction profile element is located. Between the delivery roller and the perforated apron, the condensing occurs. The roller pair functions in a classical way as in ordinary draft system. [31]

The following figure illustrates the difference between the three systems.

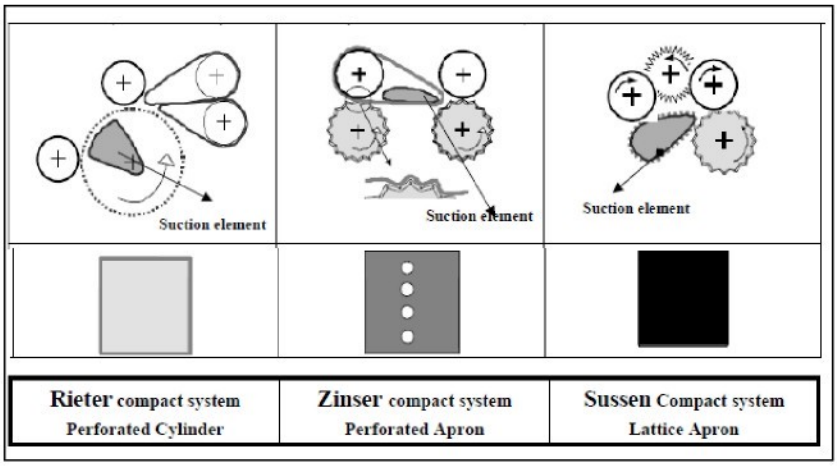

Fig. 10 Compacting systems for Rieter, Zinser and Sussen

2.5 Air-jet Spinning Techniques

The current trend and area of focus in terms of staple spun yarns is the use of air currents or an air vortex to consolidate the fibers into a yarn structure. These yarns have assumed a completely new structure when compared to conventional ring spun yarns as well as rotor yarns and are said to be a hybrid between the two. This is since the fibers do possess real twist to a certain extent, false twist and wrapper fibers. The effect is especially pronounced in the vortex spinning system that incorporates a hollow spindle. These yarns have been termed fascinated yarns, the term fasciated means bounded or compacted together, and this is what occurs to the fibers within the yarn body.

2.5.1 Development of Fasciated Yarn Technology

Spinning yarns inserting false twisting utilising an air-jet was initiated by Du Pont in 1956 [4]. The invention consisted of a number of spinning methods which included either inserting false twist to a filament bundle or a filament /staple fiber bundle by air jet nozzles and then heat setting. It was discovered that the latter method could be used to produce yarns made from 100% staple fibers with the omission of filament feeding, adhesive application, and heat setting sections. The resulting yarn was called "sheaf yarn" which consisted of staple fibers tied firmly by other staple fibers along the yarn length at random intervals.

In 1963 Du Pont introduced another method, which was particularly suitable for a tow prepared for stretch-breaking. In this method filament tows were fed into a stretch break unit, where they were broken into staple form by stretching and expanded into a ribbon shaped bundle. Subsequently an aspirating jet removed the fibers from the front rollers and guided them to a twisting jet unit. The twisting jet applied a strong torque to the fiber bundle. This torque was effective on only the core fibers. Beyond the twisting jet this twist was shifted to the surface wraps.

In 1971 Du Pont patented the "Rotofil" process, which was very similar to the process mentioned above, but in this process staple fibers were used instead of filament tows. The Rotofil process involved drafting fiber strands and forwarding them to a torque jet by means of an aspirating jet. In the torque jet the fibers were consolidated into a fasciated yarn assembly by twisting. The drafted fiber bundle was presented to the aspirating jet as a "spread out" web. The torque applied by the torque-jet mainly affected the core part and the "edge fibers" (i.e. those fibers at the outside of the strand) took less twist compared to the fibers at the center.

The yarn consequently consisted of highly twisted core and less twisted surface fibers as it entered the air jet. When it left the air-jet unit, the surface fibers became untwisted first and then twisted in the reverse direction, while the core fibers continued to be untwisted. The resultant yarn consisted of surface fibers wrapped around core fibers at varying helix angles ranging from about 10° to 80°. This process was suitable for staple

fibers ranging from 50 mm to 350 mm in length. Mainly acrylic fibers were used in the Rotofil process, and the resultant yarn was called “Nandel”.

Although Du Pont was the first pioneer in fasciated yarn technology, none of Du Pont’s systems has achieved commercial success, and they have been abandoned due to economic reasons and the inadequate properties of yarns produced by these systems. However, the idea has been further developed by a number of machine builders including Toray Engineering Ltd [26], Toyoda Automatic Loom Works Ltd., Howa Machinery Co., Suessen [13], and Murata Machinery Ltd [19]. Among them only Murata has achieved real commercial success with their MJS air jet system that was launched in 1981 and the Murata vortex system that was launched in 1998.

2.5.2 Ring-jet spinning

This entails the incorporation of an air-jet positioned after the front roller nip on a conventional ring frame. The fibers during the spinning operation are subjected to both false twisting by the air-jet and real twisting by the rotating spindle. A consolidation effect is imparted to the fibers by the air-jet, as well as the creation of wrapper fibers. The flow of the air within the jet is as in air-jet spinning. The spindle imparts real twist and winds on the resultant yarn. See Figure 11.

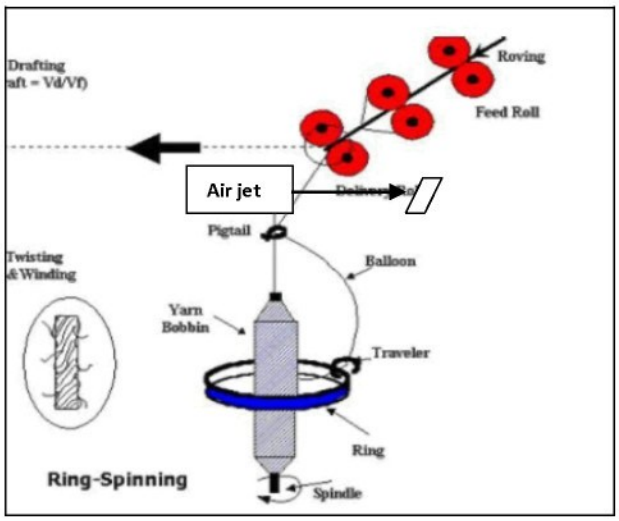

Fig. 11 Ring-jet spinning

The direction of the air-flow in the air-jet can be either towards or away from the front roller. Since twist is propogated from the traveler upwards, edge fiber protrusions are towards the front roller. Hence air flow in that direction will facilitate their incorporation into the yarn body. The dynamics of the air flow in the jet is as explained for air-jet spinning below.

The air-jet induces an upward swirling air flow against yarn movement. Barella [3] and Pillay [22] have found that most of the protruding fiber ends correspond to fiber tails for ring spun yarns. Therefore, an air flow in the direction of yarn movement may promote rather than suppress these protruding fiber ends. Furthermore, since the swirling air current in the jet twists the yarn strand in the reverse direction, the twist level in the strand above the jet is lower than that in the strand below the jet. Therefore as the fiber strand traverses through the jet, the structure first gets loosened to some extent and then tightens up again as it emerges from the jet. This loosening and tightening up of the strand structure may facilitate in tucking of the fiber ends into the body of the yarn, thus effectively reducing the hairiness.

Kalyanaraman [11] found that by increasing the pressure of air around the point of twisting, the yarn hairiness can be significantly reduced. With the present ring-jet arrangement, it is expected that the combined effects of swirling air, reverse twisting and air pressure would lead to an effective reduction in yarn hairiness without adversely influencing the other yarn properties. His study also shows that the hairiness level in ring spinning of cotton yarns considerably decreases with the employment of a pressure column in-between the front roller nip and the lappet hook.

Wang, et al. [27] achieved reduction in hairiness of yarn by the upward swirling air against the yarn movement and twist, which facilitates the tucking of protruding fibers into the body of the yarn by loosening and tightening up of the fiber strand. Hence, the utility of air jet has to be considered with serious interest in view of its immense potential in influencing the surface properties of yarn. The air ring spinning system combines air jet and ring spinning technologies. Cotton being a finer and shorter fiber would present more ends per unit length, which increases the number of fibers protruding out of the yarn surface and affects its surface and structural properties.

2.5.3 Air-Jet Spinning

The classical air-jet spinning uses the principle of false-twisting to produce a yarn of uniquely different structure from that of ring or rotor spun yarn. While ring-spinning is characterised by a continuity in the fiber flow, and rotor spinning is characterised by a complete separation of fibers prior to spinning, air-jet spinning exhibits an intermediate feature in which part of the fiber strand flows continuously and another part is separated.

The Murata Jet Spinner, the MJS 801, was introduced by Murata at ATME' 82. This system consists of a three-line drafting device and two contra-rotating nozzles. The consolidation mechanism in air-jet spinning is achieved by blowing out compressed air through air nozzle holes of about 0.4mm diameter to form an air vortex.

Feed is in the form of drawframe sliver that is passed through a drafting system and the delivered fiber web, which is in a broad-spread form as it leaves the nip line, advances to air-nozzles located directly after the drafting device. The first nozzle which provides airflow in the opposite direction with a weaker intensity than the second nozzle does not affect the core fibers but prevents the edge fibers in the spinning triangle from being twisted in, or twists them in the opposite direction around the core fibers.

The second nozzle imparts a false twist to the fiber bundle that travels back to the front rollers of the drafting unit. Therefore, only the core part, which is the main part of the fiber bundle, is influenced by the second nozzle. Edge fibers either do not have twist or have little twist. When the fiber strand departs the second nozzle, core fibers no longer exhibit any twist. They are arranged in parallel form. On the other hand, edge fibers receive true twist in the opposite direction to that of the upstream twist and wrap around the nearly parallelcore fibers [13,16,20]. The principle of this system is shown in Figure 13. and the twist distribution during yarn formation shown in Figure 12.

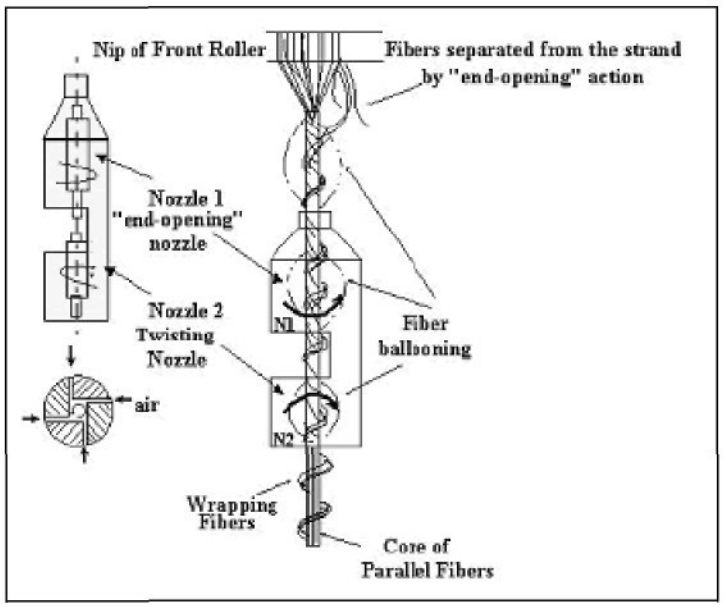

Fig. 12 Operating principle of Murata Air-jet Spinning Machine

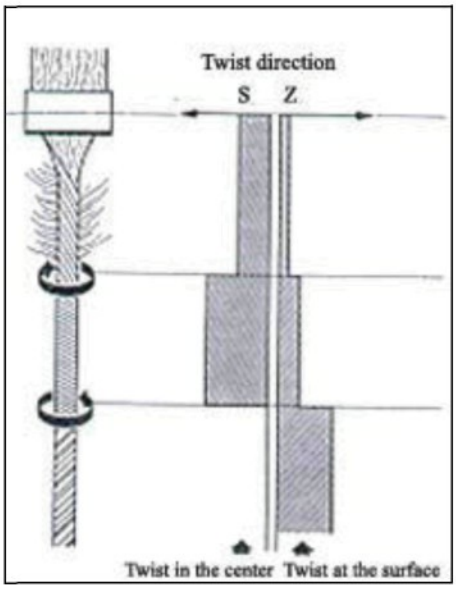

Fig. 13 Twist Distribution During Yarn Formation

At the time the MJS 801 was introduced, its delivery speed was 160 m/min, ten times faster than that of ring spinning and was capable of spinning finer yarns than the rotor system [16]. As a result of these advantages, the MJS 801 system rapidly captured commercial success in spinning pure synthetic fibers, blends of synthetic fibers, or rich

blends of synthetic with cotton fibers. However, it is not suitable for pure cotton fibers or rich blends of cotton fibers. The only way to process 100 % cotton fibers is to use combed form, which still results in a lower yarn strength compared to ring yarns [13]. High energy costs associated with high consumption of compressed air due to two nozzles, and difficulty in obtaining regularly wound wrapper fibers when the fiber length increases owing to unstable ballooning during spinning were the shortcomings of the system. In the late 80's Murata introduced a new version of this system, the MJS 802 [4].

The MJS 802 comprised of a 4-line drafting unit and a modified nozzle which provided better yarn control. Production speeds were also increased to 210 m/min, and was claimed to spin 100% cotton [30]. Murata later launched two other new air-jet spinning systems: the 802H [6,7] and 804 RJS [1,8] with production speeds of up to 300 m/min and 400m/m, respectively. The 802H system consists of the following: a 5-roll drafting system, which allows spinners to use even coarse slivers at high speeds, the grooved-front top cots for better air flow control at high front roller speed, and a modified nozzle to assist high speeds, which was positioned closer to the drafting unit to minimize ballooning [8]. The design features of 804 RJS were similar to the 802H except that the second nozzle was replaced with a set of rubber-covered balloon rollers. This new feature claimed a reduction in energy use and yarn hairiness and resultant yarn having a more ring-spun like structure and appearance [8,16]. The 804 RJS has not however proven to be a commercial success.

2.5.4 Air- Vortex Spinning

Vortex spinning technology, the most recent of innovations in the field of air-jet spinning, was also developed by the Japanese firm Murata (Muratec). Murata's No. 851 Vortex Spinner made its first appearance at OTEMAS'97. [19] Vortex spinning is a false twist process, and the twist insertion in this system is achieved by means of air-jets. The main attraction of vortex spinning is that it is claimed to be capable of spinning 100% carded cotton fibers at speeds of up to 400m/min, and the resulting yarn structure is more comparable to ring yarn than to rotor yarn [2,6,8].

Other claimed advantages of vortex spinning are a low maintenance cost due to fewer moving parts, elimination of the roving frame stage, and improved fully automatic

piecing system. In addition to these, yarns produced by this method have low hairiness compared to normal ring yarns. This is claimed to be due to being “air-singed” and “air-combed,” which in turn results in reduced fabric pilling; and fabrics made from vortex yarns have outstanding abrasion resistance, moisture absorption, color-fastness and fast drying characteristics [2]. Murata suggests that MVS is best suited by far to the high volume production of medium cotton yarns from carded cotton.

One of the major setbacks of this spinning technology is the high speed drafting. In this system the drafting unit has to operate at a speed 10 times higher than in the case of ring spinning. Other major problems are the fiber loss during spinning and the frequent contamination in the jet nozzles since fiber material may be fed to the spinning unit without being adequately cleaned, by combing for example.

2.5.4.1 Principle of Vortex Spinning

Sliver is fed to a 4 roller drafting system and the emergent drafted web is sucked into the fiber bundle passage by air suction created by the nozzle. The fiber bundle passage consists of a nozzle block and a needle holder. The needle holder has a substantially central, longitudinal axis and a guide surface that twists relative to the longitudinal axis, see Figure 14. A pin-like guide member associated with the needle holder protrudes toward the inlet of the spindle.

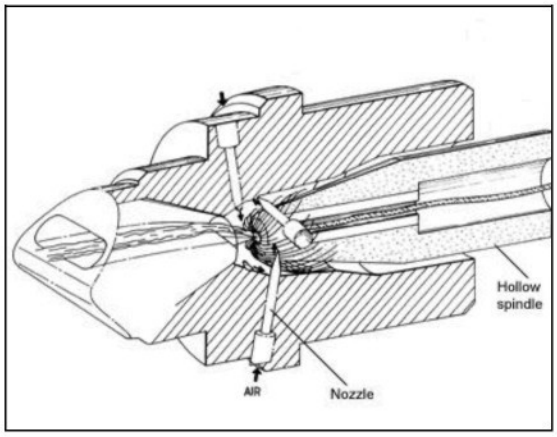

Fig. 14 Air-vortex spinning unit

Fibers are smoothly sucked into a hollow spindle and twist insertion starts as the fiber bundle receives the force of the compressed air at the inlet of the spindle. The twisting motion tends to propagate from the spindle toward the front rollers. This propagation is prevented by the guide member that temporarily plays a role in the center fiber bundle. After fibers have left the guide member, the whirling force of the air jet separates fibers from the bundle. Since the leading ends of all fibers are moved forward around the guide member and drawn into the spindle by the preceding portion of fiber bundle being formed into a yarn, they present partial twist and are less affected by the air flow inside the spindle. Conversely, when the trailing ends of the fibers which have left the front rollers move to a position where they receive the whirling force of the nozzle, they are separated from the fiber bundle, extend outwardly and twine over the spindle. Subsequently, these fibers are spirally wound around the fiber core and formed into a vortex spun yarn as they are drawn into the spindle. See Figure 15 and 16 [6].

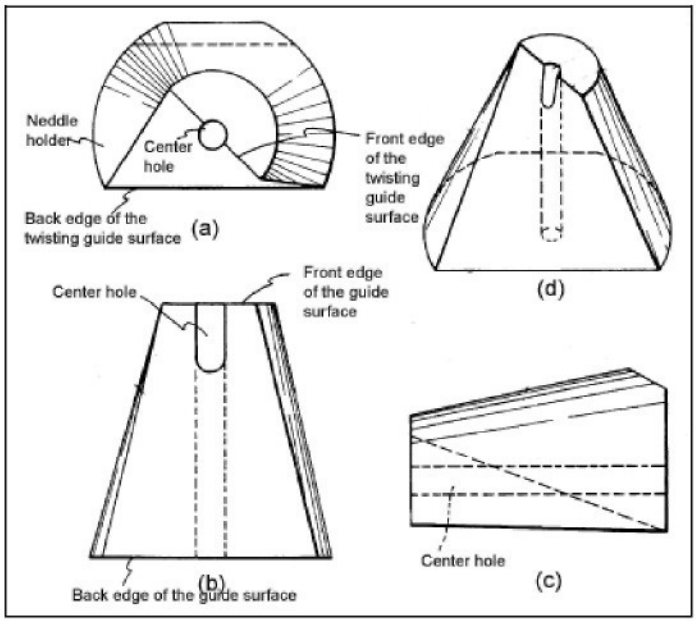

Fig. 15 (a) plan view, **(b)** front view, **(c)** side view, and **(d)** perspective view of the needle holder.

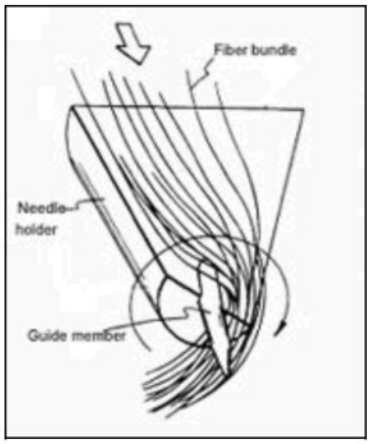

Fig. 16 Needle holder with the guide member.

The finished yarn is wound on a package after its defects have been removed. During the yarn formation, most of the fibers are not false twisted since the twist propagation is prevented by the guide member, and the fiber separation from the bundle occurs everywhere in the entire outer periphery of the bundle. This results in a higher number of wrapper fibers in the yarn, explaining why vortex spun yarns present much more wrapper fibers than air-jet spun yarns, and their yarn structure is similar to ring yarns [15,49,64]. Figure 17 represents an idealised structure of vortex spun yarn.

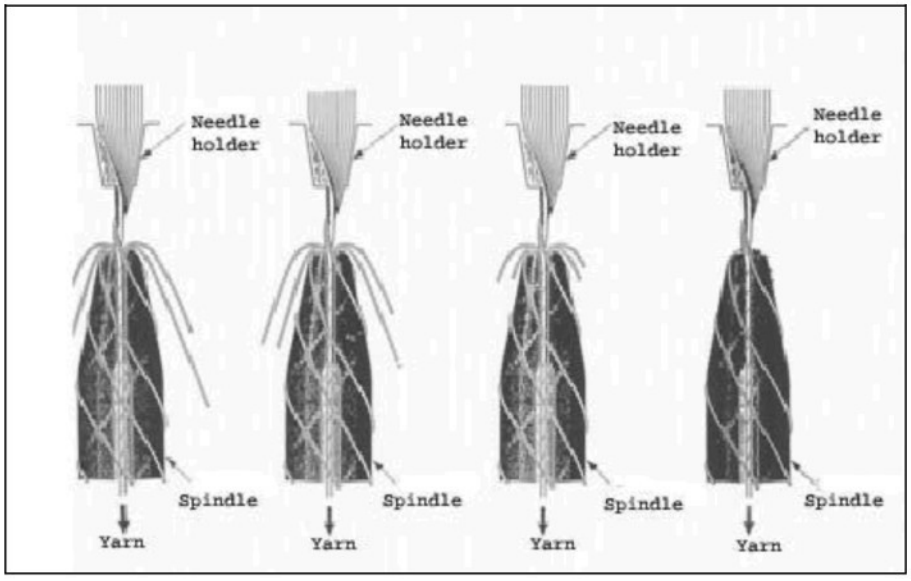

Fig. 17. Yarn formation in vortex spinning [15]

2.6 Classes of Air-Jet Yarns

The figures below depict the structure of the four different classes of air-jet spun yarns. The classes 1-3 are produced from conventional air-jet spinning and class 4 from air vortex spinning. It can be seen the manner in which the fibers arrange themselves in the yarn structure. Class 4 produced from air vortex shows a high degree of wrapper fibers, arranging themselves in a three dimensional manner as compared to classes 1-3.

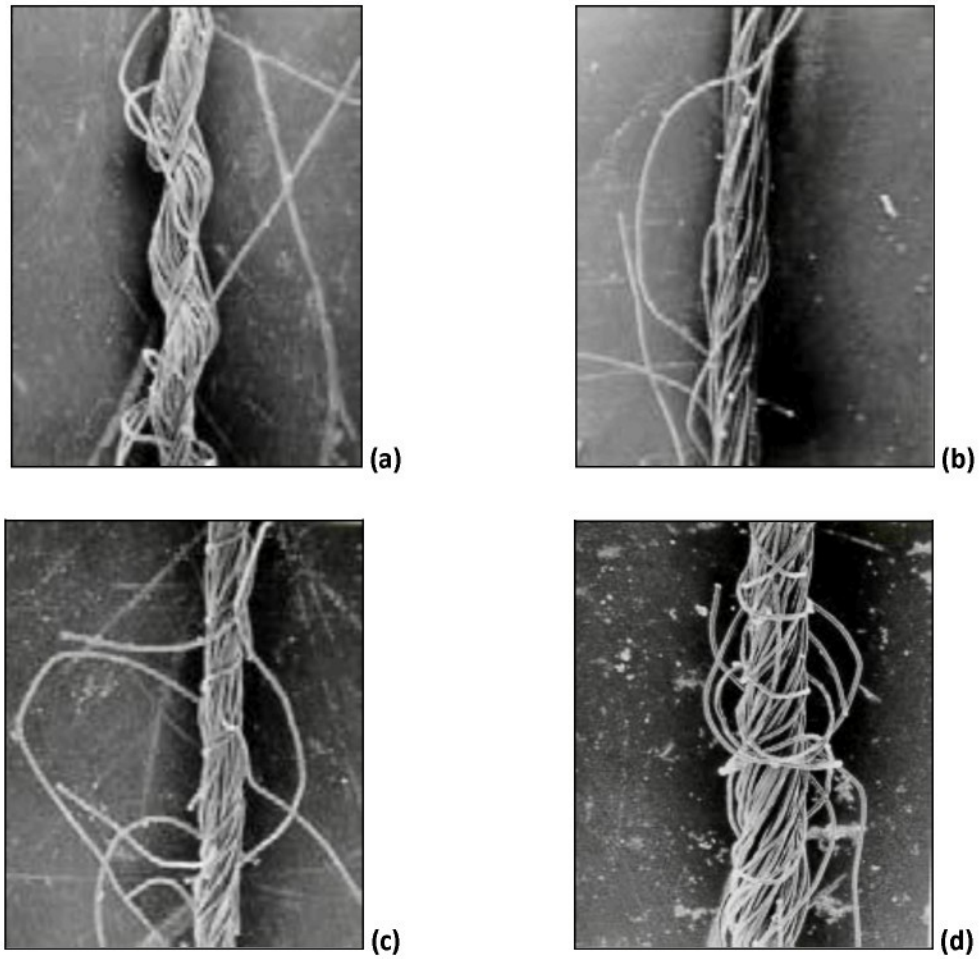

Fig. 18 Classes of air-jet yarns **(a)** Class 1 **(b)** Class 2 **(c)** Class 3 **(d)** Class 4

2.7 Investigations conducted on air spinning techniques

2.7.1 Effect of jet-ring spinning on yarn hairiness

The effect of spindle speed, air pressure, twist and distance of the jet from the nip point of the roller was investigated by Cheng , K and Li, S [5]. The trials were conducted both on cotton and polyester. In comparison to conventional ring spun yarns a reduction in yarn hairiness of 41% was obtained for cotton yarns and 26 % for polyester yarns.

The correlation between air pressure and yarn hairiness was strong for cotton yarns and with an increase in air pressure from 0.5 to 2 bars showed a reduction of 20% in hairiness. The correlation between air pressure and hairiness was, however not as strong for polyester. Both cotton and polyester yarns showed reduction in yarn hairiness with increasing spindle speeds. It was noted that in general, the hairiness of the cotton yarn was lower than that of polyester at the same spindle speed.

A strong correlation for both yarn types was obtained in terms of yarn twist, and increasing twist levels resulted in a decrease in yarn hairiness. A 20% decrease with an increase in 1.0 of a twist factor. The effect of distance of the air jet nozzle from the front roller on yarn hairiness was however found to be insignificant.

The findings here suggested that the incorporation of an air-jet nozzle below the front roller nip, impacted significantly on the yarn hairiness levels. This is probably due to the hypothesis that the yarn structure is loosened as it enters the nozzle, and the subsequent tightening up of the structure, as it emerges from the nozzle may tuck or wrap protruding fiber ends in the yarn body due to the swirling air current induced by the air-jet nozzle.

Since most of the protruding fiber ends are trailing [3,22], the axial air vortex spiralling along the yarn in a direction opposite to that of the yarn twist may suppress rather than promote these fiber ends. When wrapper fibers increase beyond a certain amount, they are expected to bind the yarn and decrease the protrusion of fiber ends, resulting in a decrease in yarn hairiness [27]. In comparison to conventional ring spun yarns, better yarn tenacity and breaking force has also been achieved. Fiber properties do however play a significant role in influencing the effectiveness of the wrapping action [5].

2.7.2 Jets using air vortex in direction and opposite to yarn twist

Ramachandralu,K and Dasaradan, B [23] used two types of air jet nozzles, differing from each other in the direction of inclination of orifice and suitability for air vortex ring spinning system. The drafted cotton fibers emerging from the front roller nip passes through the air jet nozzle is subjected to the action of the air vortex of compressed air, which tucks the protruding fibers, and subsequently as the yarn emerges from the nozzle, they are bound by the mechanical twisting action, thereby reducing the yarn hairiness.

The performance of these two types of nozzles, one producing an air vortex in the direction same as that of yarn twist, i.e, in Z direction and the other in the direction opposite to that of yarn twist, i.e, in S direction, was evaluated on *30 s* carded yarn spun under 0.5 bar compressed air. The design of the nozzle is shown in Fig. 14 below.

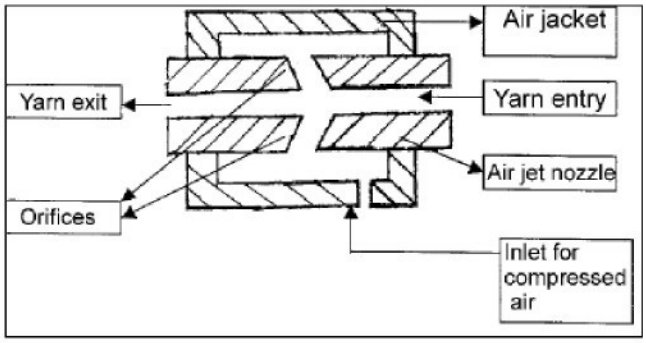

Fig. 19. Design of air-jet nozzle assembly [5]

It was observed that the best results were achieved with the air jet nozzle, where the direction of rotation of the air vortex created was in the same direction as that of the yarn twist. Using this nozzle, hairs in the yarn decreased by 50% at 0.5 bar air pressure, a 11.5% decrease in imperfection level and a marginal increase in strength.

This is as a result of the fact that ring spun yarn has more fiber ends protruding in the trailing direction [3,22]. When the yarn passes through the nozzle it encounters the air vortex created by the upward swirling air current, gyrating in the opposite direction. In case of the nozzle with the Z direction, the air vortex false-twists the partially twisted yarn in the direction same as that of yarn twist, i.e, in Z direction which is schematically shown in Figure 15. This air vortex produced by the upward swirling air current tucks the

protruding fibers, particularly the trailing hairs, onto the yarn surface. When the yarn comes out of the nozzle the tucked hairs are bound into the yarn structure as the mechanical twist created by the revolving traveller flows towards the nozzle. The sweeping action of the air vortex, which effects in the realignment of the fibers, contributes greatly to reduced hairiness [23].

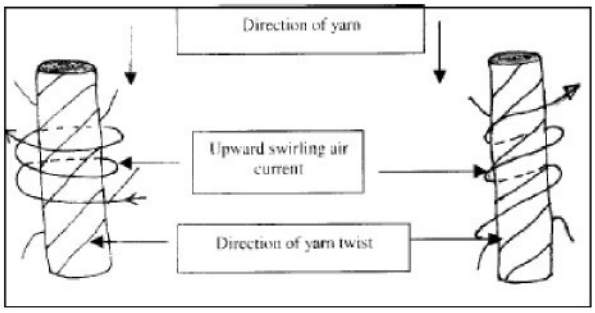

Fig. 20 Air-flow directions [23]

In the case of the nozzle having the opposite direction, the air vortex produced by the upward swirling air current false twists the partially twisted yarn in the direction opposite to that of yarn twist, ie, in S direction, which is shown schematically in Figure 4. The upward swirling air current against the movement of yarn and twist, loosens the fiber strand. As the yarn comes out of the nozzle the loosened fiber strand gets tightened by the flow of twist from the mechanical twisting agency, when by the binding of the tucked fibers takes place as explained by Wang, et al [28] in their study of air jet spinning. The reason for achievement of better reduction with first nozzle could be due to the better wrapping of protruding fibers by the sweeping and binding action of the air vortex current twisting the strand of fibers in the direction same as that of the yarn twist.

2.7.3 Air Flow in the Air-jet False-twist Spinning Chamber

The air flow in a false-twist spinning chamber operating according to the MJS (Murata Jet Spinning) principle was investigated by Witczak, D. and Golanski, J., [28] in the form of two variants, viz.for the chamber itself (without yarn) and during spinning. Two air jets are supplied to the swirl chamber, namely:

- the primary air jet – swirled, affected by four tangent nozzles that are supplied with compressed air of the pressure equal to p_n = 0.7 MPa and the mass flow rate m_n = 0.94·10-3 kg/s,
- the secondary air jet – the mass flow rate m_i = 0.28·10-3 kg/s.

The process parameters were as follows:

- air supply pressure p_n = 0.7 MPa,
- yarn delivery velocity v_d = 2 m/s,
- yarn linear mass 36 tex,
- yarn made of polyester + cotton (50% PET / 50% cotton - E50B50),
- draft ratio D_r = 0.966.

These jets were mixed in the swirl chamber in such a way that the swirled jet of the total mass flow rate, equal to m_f = 1.22·10-3 kg/s, flows through the swirl chamber. The outlet of the air from the chamber is free through the cylindrical part of the diameter *d3* > *d2*. In order to visualise the flow in the chamber, distributions of air velocity components determined in measurement planes 1 – 3, denoted on the schematic view in Figure 21(a), are presented.

In Figure 21(b), an air velocity distribution in the inlet channel c_i is shown. A considerable sub-atmospheric pressure in the neighbourhood of the chamber axis causes the air jet to flow into the chamber at a significant velocity of 240 m/s. The swirl of the primary jet is not transferred to the secondary jet, and the velocity direction is consistent with the chamber axis.

In Figure 21(c), distributions of air velocity components, circumferential c_c and axial c_z, in plane 2 are presented. The circumferential component distribution c_c is typical of the forced vortex with the maximum at the wall and decreasing linearly to the chamber axis. The distribution of the axial component c_z indicates that a return flow of the air jet exists, which is characteristic of swirl flows, in the neighbourhood of the chamber axis. This indicates a high mixing intensity of the primary and secondary jets so that eventually there is a homogeneous, swirled jet of the mass flow rate m at the end of the cylindrical part of the diameter d_2. The value of the maximum resultant air velocity c at the wall is

slightly higher than the sound velocity (1.06 Ma), which shows that the air in the supply nozzles reaches the sound velocity, and so the flow in this supply zone is supersonic.

In Figure 21(d), a distribution of the air velocity components, circumferential c_c and axial c_z, in plane 3 is given. Plane 3 is situated at the beginning of the cylindrical part of the diameter d_3. A flow from plane 2 to plane 3 is typical of all swirl chambers, with a characteristic change in the profile and a value of the air velocity that follows from the restructuring of the enforced vortex into a free one.

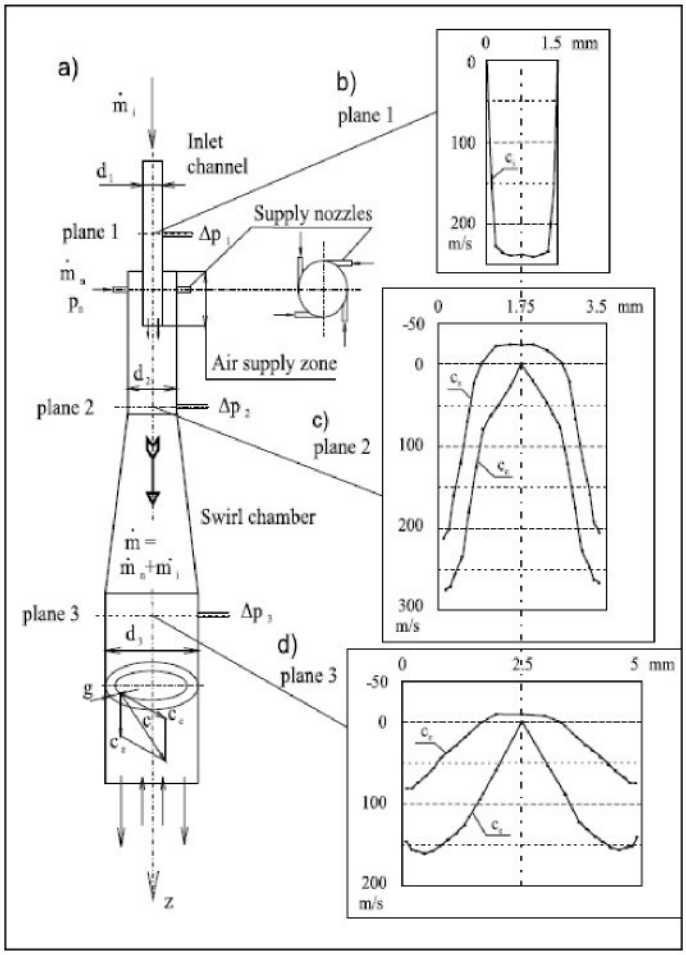

Fig. 21 Schematic view of the chamber under investigation measurement planes and air velocity distributions; a) schematic view of the spinning chamber; b) air velocity distribution in the inlet channel plane 1; c) air velocity distribution in the chamber, plane 2; d) air velocity distribution in the chamber [28].

2.7.4 Controlling the air vortex twist in air jet spinning

In the model of the air vortex twister as shown in Figure 21, compressed air is forced into the twisting chamber from the air reservoirs through the jet orifices. The air vortex then twists the fibers.

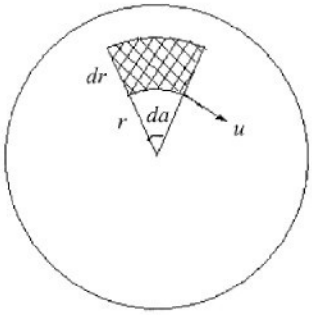

Fig. 22 Momentum on an infinitesimal area on a section of the nozzle

The system must however obey the basic laws of mechanics therefore the momentum in the horizontal direction as depicted in Figure. 22, ignoring energy loss is given as:

$$N\pi\left(\frac{d}{2}\right)^2 \rho\, \mu_0 cos\theta\, \frac{D-d}{2} = \int_0^{2\pi} \int_0^{D/2} \rho\mu r^2 2dr d\alpha \qquad (1)$$

Where ρ, is the air density, μ_o is the velocity at the jet orifice, μ is the vortex velocity, D and d are the diameters of the nozzle and orifice, respectively, θ is the orifice angle and N the number of orifices. Assuming that the flow is incompressible, the above equation becomes:

$$\int_0^{D/2} \mu r^2\, dr = \frac{N}{16}(D-d)\mu_0 \cos\theta \qquad (2)$$

Based on many experimental data and numerical analyses, we assume that the vortex velocity can be approximated as:

$$\mu = kr^n \qquad (3)$$

where k and n are constants. Substituting (3) into (2) we obtain:

$$k\frac{1}{3+n}\left(\frac{D}{2}\right)^{3+n} = \frac{N}{16}(D-d)d^2\mu_o cos\theta \qquad (4)$$

The two constants k and n can be determined by experimental data or numerical analysis. Here, we also make an approximation of the value of *k*. Assuming that the vortex velocity at r=(D-d)/2 remains unchanged through the nozzle i.e.,

$$\mu(r)|_{r=\frac{D-d}{2}} = \mu_0 cos\theta \quad (5)$$

In view of Equation 3, we identify k with ease:

$$k = \frac{2^n \mu_0 cos\theta}{(D-d)^2} \quad (6)$$

After identifying the value of *k*, n can be readily determined from Equation 4.

The strength of the vortex twist acting on the yarns can be expressed as:

$$T = \mu d_y \frac{\partial \mu}{\partial r}|_{r=D/2} = \beta d_y kn\left(\frac{D}{2}\right)^{n-1} \quad (7)$$

Where β_v is the air viscosity and *dy* the yarn diameter. The velocity μo in these equations can be experimentally determined or approximated by applying the Hagen-Poisseille formulation as well.

It was noted from the above that the strength of the vortex twist T is a function of nozzle pressure, flow rate, jet orifice angle, and jet orifice diameter. Therefore a design formulation is obtained to optimise nozzle structure. This analytical model has wider applications in processes such as air texturing, vortex spinning and air splicing.

2.7.5 Bead Elastic model

The fiber motion in the nozzle is a two phase flow situation. The high speed air inside the nozzle is the fluid phase, and the fibers constitute the particle phase [3]. Fibers however do differ from the general particulates by properties such as large aspect ratio, elasticity and flexibility. Any section of a fiber may bend, or rotate relative to the other sections due to the non-uniform flow in the nozzle.

The bead elastic model was used since it is applicable to high speed air flows such as that in the nozzle. The fiber is considered to be a chain of n beads connected by n-1 mass less rods, as shown in Figure 23. The chain is elastic and flexible, for it can stretch

by changing the distance between the adjacent beads, and can bend by changing the bending deflection in successive rods.

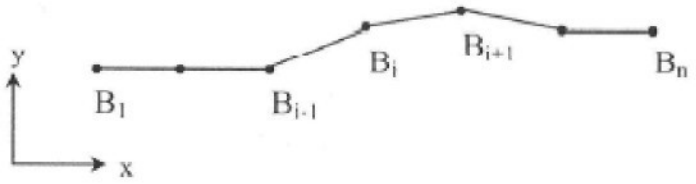

Fig. 23 Schematic of fiber model

The disposition of the beads *i* of the fiber is depicted in Figure 24. Bead *i* is adjacent to bead *i* -1 and *i* +1 only, so bead 1 and bead *n* respectively work as leading and trailing beads. The mass m_i of bead *i* is defined as

$$m_i = \frac{\rho_f}{2}\left(l_{i-1,1} + l_{i,i+1}\right) \quad (1)$$

Where ρ_f is the fiber linear density, $l_{i-1,1}$ is the sectional length of the fiber section (*i* -1,*i*), and $l_{i,i+1}$ the sectional length of the fiber section (*i* +1,*i*).

If a pair of adjacent beads *i* – 1 and *i,* which form a fiber section (*i* -1,*i*). If the distance between them is stretched, the following force F_{ei} exerted on bead *i* is:

$$F_{ei} = -k\Delta l \quad (2)$$

Where Δl is the extension of the section and *k* is a constant related to the elastic modulus E of the fiber. The direction of F_{ei} is in the direction of the fiber section.

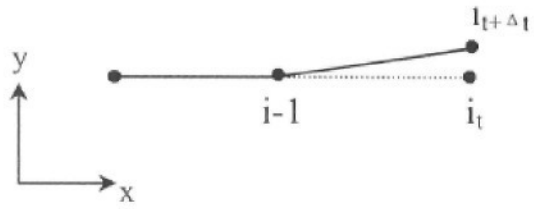

Fig. 24 Sketch of fiber bending

In Figure 24, assuming (i -1,i_t) is the equilibrium position of fiber section (i -1,i), when bead i moves from i_t to $it+\Delta t$, the fiber section is bent, so a restoring force F_{bi} is exerted on bead i:

$$F_{bi} = -B\Delta y \tag{3}$$

Where Δy is the bending deflection of the section, and B is a constant related to the flexural rigidity of the fiber. The direction of F_{bi} in this case is normal to the fiber section.

When under the influence of the air stream, the fiber is immersed in it and is subjected to air drag, which is the sum of frictional drag and pressure drag. The drag for the bead i is contributed by sections (i +1,i) and (i -1,I and may be calculated by:

$$F_{di} = \frac{1}{2}\left(F_{di-1,i}{}^{i} + F_{di,i+1}{}^{i}\right) \tag{4}$$

where F_{di} is the drag exerted on bead i, $F_{di-1,i}{}^{i}$ is the frictional drag on the bead contributed by section (i -1,i) and $F_{di,i+1}{}^{i}$ is the drag on bead i contributed by section (i,i +1). For section (i -1,i), the drag can be written as:

$$F_{di-1,i}{}^{i} = F_{fi-1,i}{}^{i} + F_{pi-1,i}{}^{i} \tag{5}$$

In which $F_{fi-1,i}{}^{i}$ is the frictional drag on section (i -1,i) and $F_{pi-1,i}{}^{i}$ is the drag on section (i -1,i) for bead i.

In order to calculate the drag on a fiber section, the local relative velocity between the air and the fiber was resolved into two components, viz. axial and normal to the fiber. The friction drag and the pressure drag on section (i -1,i), can be expressed as :

$$F_{fi-1,i}{}^{i} = {}^{1}/_{2}\, C_f \rho A_{ti-1,i} v_{rti}{}^{2} \tag{6}$$

and

$$F_{pi-1,i}{}^{i} = {}^{1}/_{2}\, C_p \rho A_{ni-1,i} v_{rni}{}^{2} \tag{7}$$

where ρ is the air density, $A_{ti-1,i}$ refers to the surface area of the fiber section, and $A_{ni-1,i}$ is the maximum cross-section area of the fiber section. At bead i, v_{rti} and v_{rni} are the

relative velocities in axial and normal direction to the fiber direction, respectively. The relative velocity is calculated as :

$$v_{ri} = v_{ai} - v_{fi} \tag{8}$$

in which v_{ai} and v_{fi} are the air and fiber velocities at the bead. C_f and C_p are the friction drag coefficients and the pressure drag coefficients respectively.

The air in the nozzle may be regarded as an isentropic flow [20], so that the energy equation is neglected. The fiber motion model is governed by the following equations:

The air phase:

$$\frac{\partial \rho}{\partial t} + \nabla.(\rho v_a) = 0 \tag{9}$$

$$\frac{\partial}{\partial t}(\rho v_a) + \nabla.(\rho v_a v_a) = -\nabla p + \nabla.\tau + \rho f \tag{10}$$

where p is pressure, τ is shear stress tensor, and f the body force per unit mass.

The fiber phase:

$$m_i \frac{d^2 r_i}{dt^2} = F_{ei} + F_{bi} + F_{di} \tag{11}$$

where r_i is the position of the bead *i*,, m_i the mass of the bead and F_{ei} , $F_{bi,}$ and F_{di} , the drag in the respective directions [37].

3 Experimental Part --- Ring-Jet

Yarn was produced on a conventional cotton ringframe that was modified to incorporate an air-jet. The air-jet was positioned between the front roller nip and the yarn guide as depicted in the Figure 24. The twist in the yarn, was a combination, of false -twist created by the jet and real twist created by the rotating spindle.

Material used was 100% combed cotton and supply to the ringframe was in the form of a roving of 360 tex. Resultant yarn count being 22 tex with a spindle twist of 684 turns per metre.

Two trials were conducted as listed below:

- Air flow in the direction of spindle (top-down)
- Air flow in the direction of top roller (down-top)

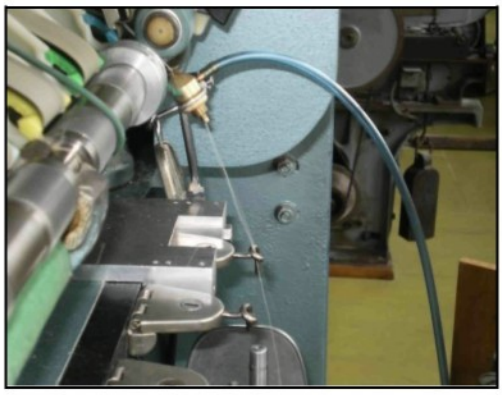

Fig. 25 Position of air-jet

The following variables were investigated:

- Position of jet from front roller.
- Air pressure.
- Number of holes in jet.

Components of the jets are shown in the figure below:

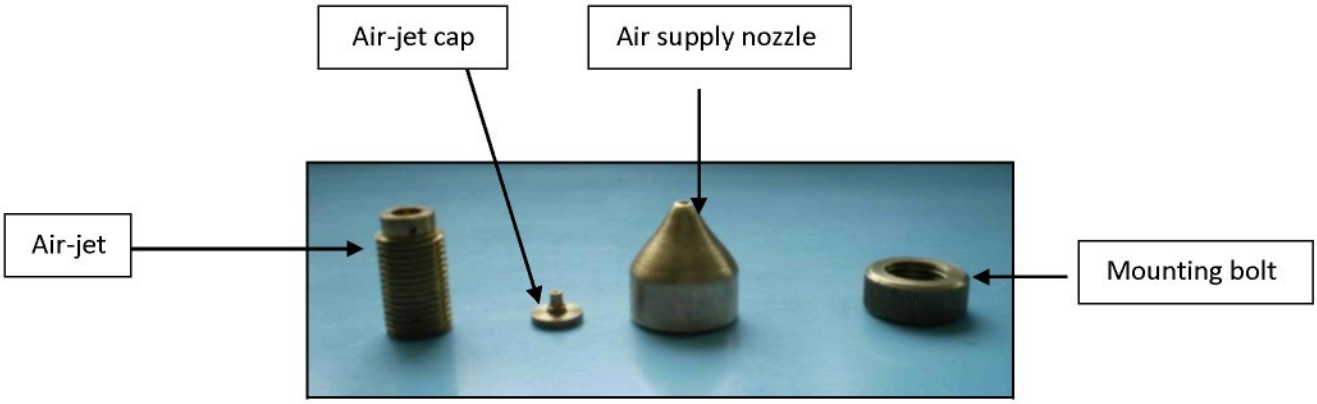

Fig. 26 Components of air-jet

For the purposes of comparison, yarn was spun on the same spindle but without the jet. The comparative results and graphs are shown on table 3 in the appendix and figures 39 to 41.

3.1 Experimental Design

The Box-Behnken experimental design was used. In this case, three factors at a time were investigated as outlined earlier, viz., air pressure in nozzle, position of the nozzle, the number of holes and quantity of air supplied. This design allows only fifteen experiments, instead of twenty seven, as in the case of using the full design. Combinations of two of the factors at two levels were taken, keeping the third at the middle value, together with three repetitions at middle value for all the variables.

Table 1 Experimental Design

Factors/Levels	Air Pressure (bar)	Nozzle Position Distance from front roller nip (mm)	Number of Holes	Quantity of air (l/min)
-1 (--)	0.25	15	2	8
0 (0)	0.50	24	3	10
+1 (+)	0.75	33	4	12

The combinations used in terms of the factors or levels are shown in table 2. In the case where the number of holes was kept constant at three and the quantity of air varied, then column three would represent it.

Table 2 Combination of factors

Air Pressure	Nozzle Position	Number of Holes/ Air flow
--	--	0
--	+	0
+	+	0
+	--	0
0	+	+
0	+	--
0	--	+
0	--	--
+	0	+
+	0	--
--	0	+
--	0	--
0	0	0

For the trial 13 experiments were conducted since only one was done with all factors at the middle level.

3.2 Evaluation of results

The test results were analyzed applying the stepwise backward regression model. The coefficients were estimated and tested against F- value, either retaining or removing them depending upon their significance. Initially all the elements were included in the model and the least significant elements of the equation are removed systematically, until all elements become significant. The generalized regression equation is given as:

$$y = \beta_0 + \sum_{i=1}^{k} \beta_i X_i + \sum_{i=1}^{k} \beta_{ii} X_i^2 + \sum_{i<j}^{k} \beta_{ij} X_i X_j$$

where β_0 is the constant of the regression equation and β_i, β_{ii} and β_{ij} are the coefficients for the elements X_i, X_i^2 and $X_i Xj$ respectively .Contour lines with the response surface were plotted for the analyzed results. It was observed that, in most of the cases the influence of the number of holes was insignificant or not having much influence. Therefore, in the plotting of the response surface and the contour lines, it was kept constant at 3 (0 level).

3.3 Testing

The yarns were conditioned for at least 24 hours under standard conditions before testing, i.e 27°C and 67%R.H. They were then tested on UT4 (Uster Unevenness Tester-4) for mass unevenness, yarn diameter and hairiness, using a test speed at 200 m/min. Tensile testing was carried out on the Instron Tensile Tester. The gauge length being 50 cm and time to break 20±3 sec. Yarn hairiness was also measured on the Zweigle hairiness tester.

3.4 Results and Discussion

3.4.1 Yarn Diameter

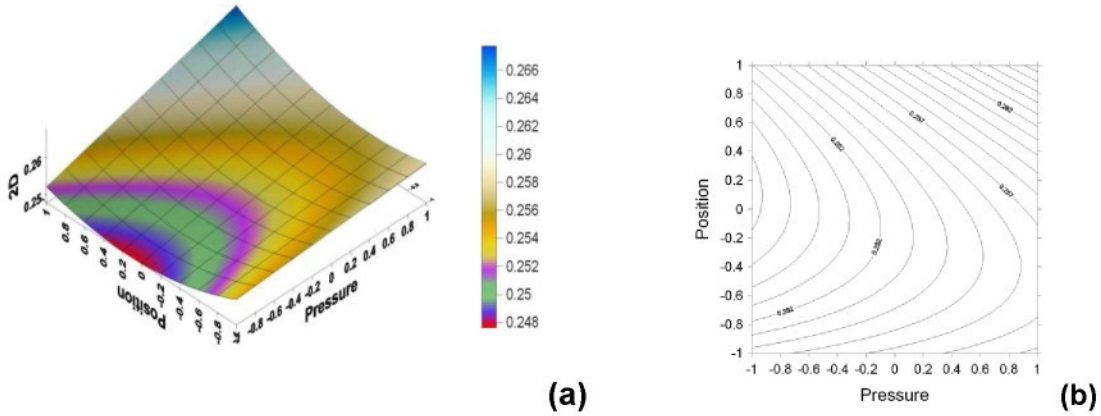

Fig. 27 Yarn diameter Vs. Position and Pressure (a) Response Surface (b) Contour Lines. Air Flow downward.

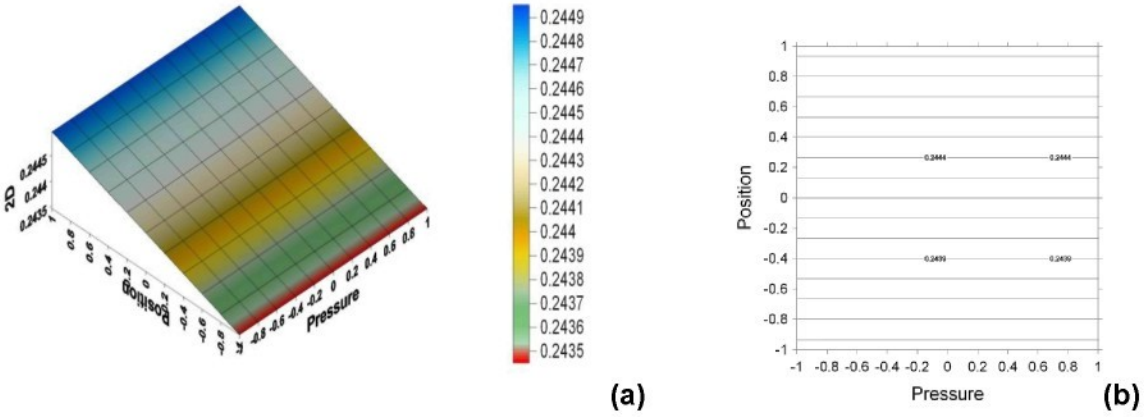

Fig. 28 Yarn diameter Vs. Position and Pressure (a) Response Surface (b) Contour Lines Air Flow Upward.

It can be seen from figure 27, representing downward air flow that the yarn diameter varies between 0.248 to 0.268 mm. The minimum diameter is obtained at a pressure of 0.25 bar and at nozzle position about 25 mm from the front roller nip. The diameter becomes a maximum at maximum pressure and position. However, with the upstream air flow, the variation in yarn diameter with change of position is barely significant. Air pressure has no influence on diameter. The values change only in the

decimal 3rd position. This can be attributed to the air pressure not being strong enough to affect the yarn diameter, which has already been set by the twist of the spindle.

3.4.2 CV% Yarn Diameter

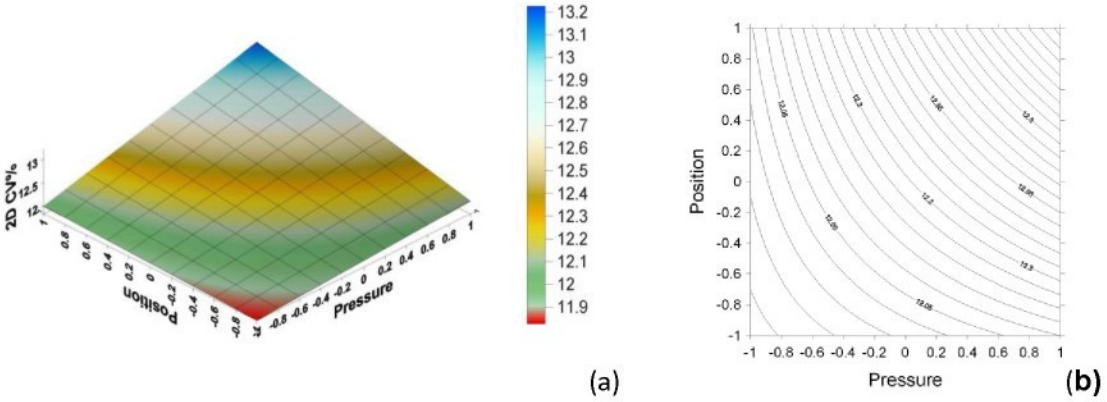

Fig. 29 Yarn diameter CV% Vs. Position and Pressure (a) Response Surface (b) Contour Lines. Air Flow Downward.

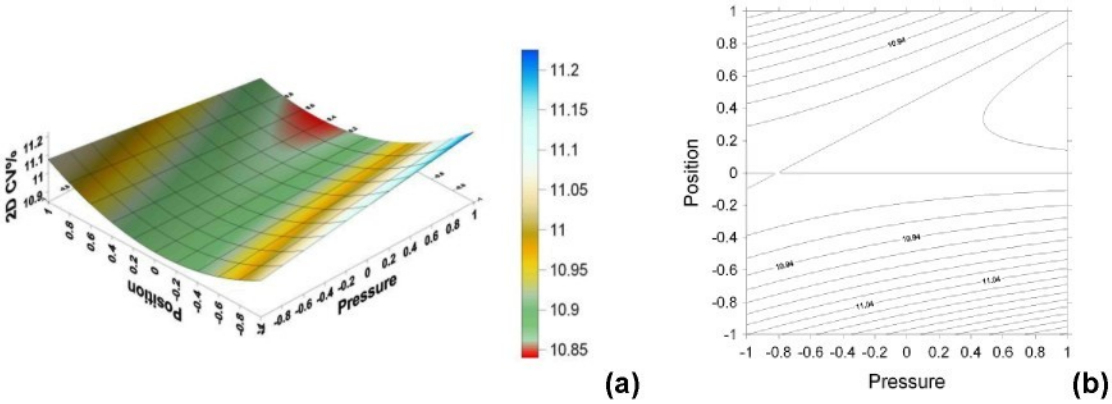

Fig. 30 Yarn diameter CV% Vs. Position and Pressure (a) Response Surface (b) Contour Lines. Air Flow Upward.

For air flow in the downward direction, the minimum value of yarn diameter CV% was obtained at minimum air pressure an position of the nozzle, viz at 0.25 bar and 9 mm from the front roller nip. See figure 29. In the case of upward air flow, the minimum was obtained at a pressure of about 0.7 bar and a distance of 23 mm of the nozzle from the front roller nip.

3.4.3 Uster CV% Mass

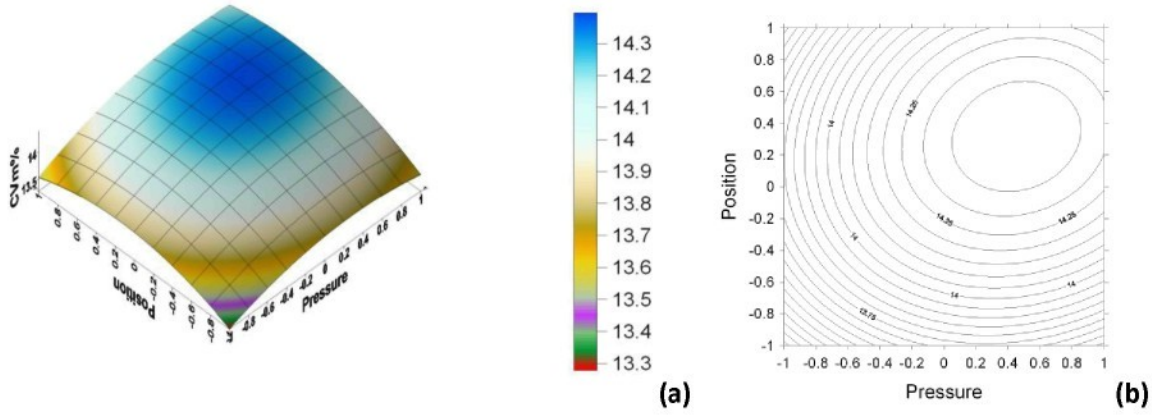

Fig. 31 Uster CV% Mass Vs. Position and Pressure (a) Response Surface (b) Contour Lines. Air Flow Downward.

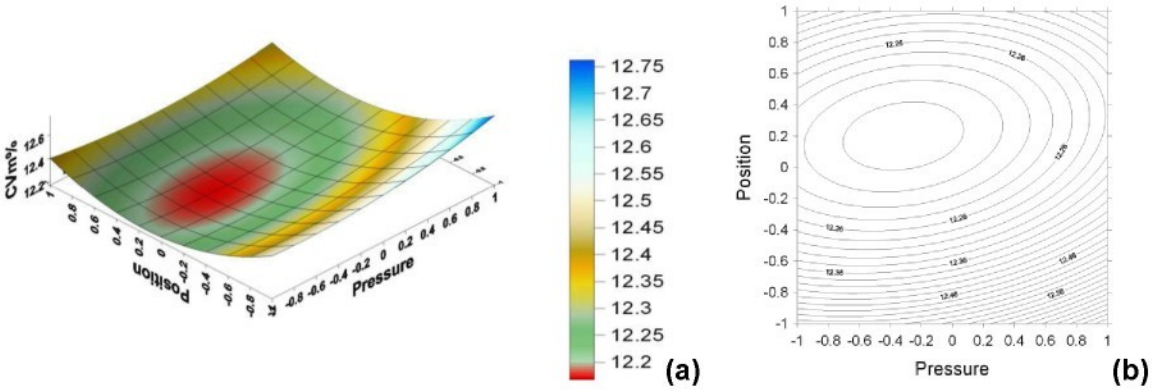

Fig. 32 Uster CV% Mass Vs. Position and Pressure (a) Response Surface (b) Contour Lines. Air Flow Upward.

The minimum value of irregularity of 13.3% was obtained at a pressure of about 0.3 bar and nozzle position of about 9 mm, as can be seen in Figure 31, where the flow of air is downstream. The yarn irregularity (CV%) ranges between 13.3 and 14.5 and reaches its maximum at a pressure about 0.6 bar and the position of the nozzle at about 28 mm from the front roller. On the other hand, where the air flows in the upward direction as in figure 31, we can recognize that the CV% ranges between 12.1 and 12.8. The minimum CV% of 12.1 was obtained at a pressure of 0.4 bar and position of 26 mm from

the nip point of the front roller. We conclude that the upstream flow produces better yarn evenness.

3.4.4 Uster Hairiness

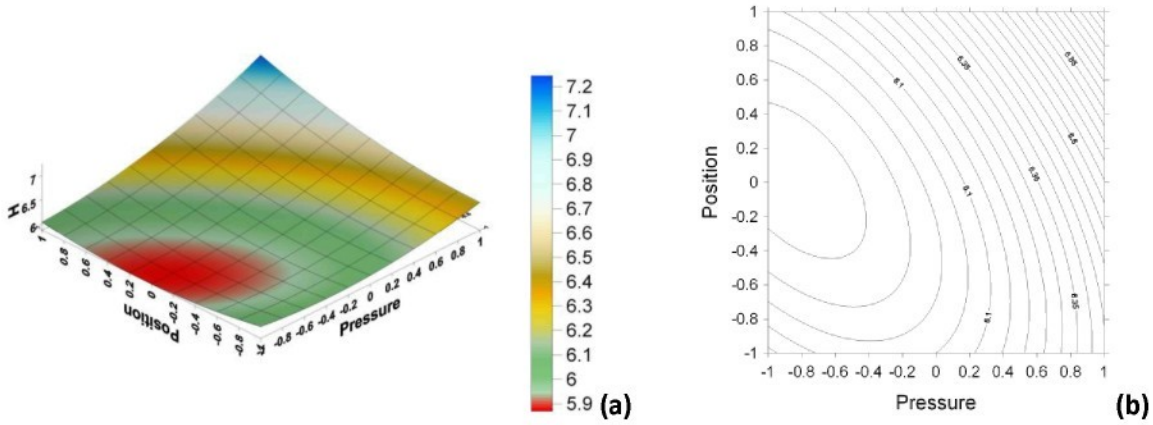

Fig. 33 Uster Hairiness Vs. Position and Pressure (a) Response Surface (b) Contour Lines. Air Flow Downward.

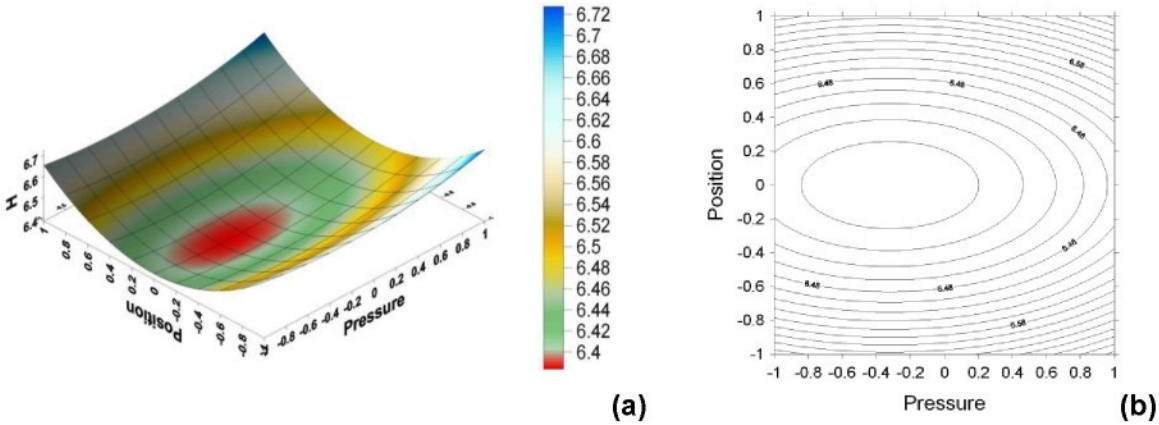

Fig. 34 Uster Hairiness Vs. Position and Pressure (a) Response Surface (b) Contour Lines. Air-flow Upward.

For the downward air flow, the minimum Uster hairiness is about 5.9 cm/1cm, and is achieved at air pressure of 0.25 bar, and nozzle position of 24mm from the nip point of the front drafting roller as can be seen in Figure 33. In case of upward airflow, the hairiness value H, ranges between 6.4 and 6.7 which is very low, however a minimum value is reached at about pressure of 0.4 bar, and distance of 19 mm from the front roller

of the drafting system. In this case, downward air flow produced a better result viz. a lower hairiness value.

3.4.5 Zweigle Hairiness

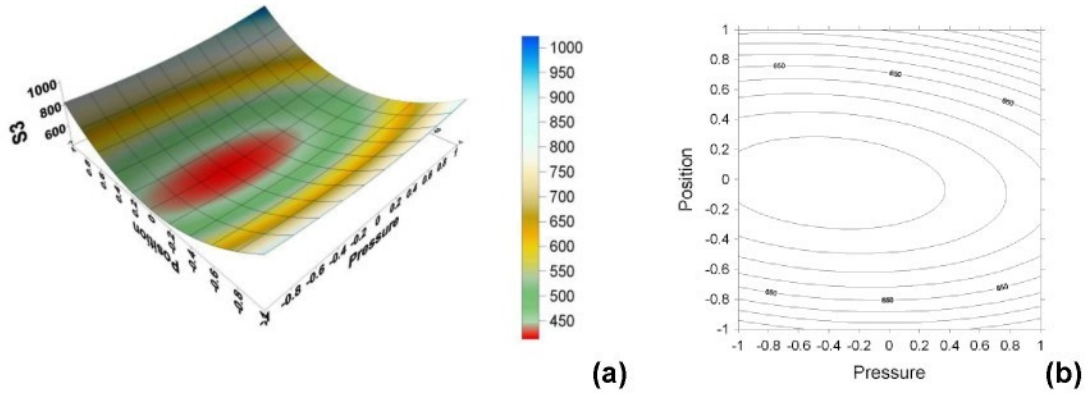

Fig. 35 Zweigle Hairiness Vs. Position and Pressure (a) Response Surface (b) Contour Lines. Air Flow Downward.

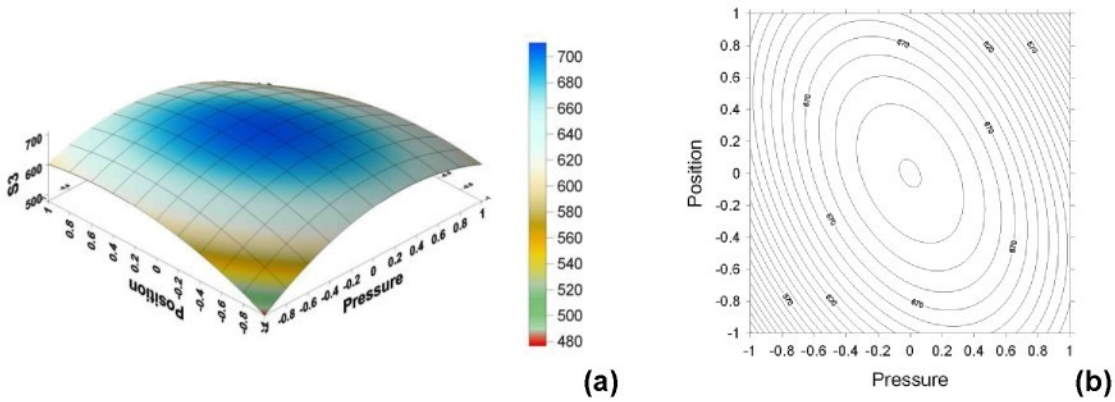

Fig. 36 Zweigle Hairiness Vs. Position and Pressure (a) Response Surface (b) Contour Lines. Air Flow Upward.

From Figure 35 we can see that the number of hairs S3, i.e. the total number of hairs of 3mm and more ranges between 440 and 1000. The minimum number of hairs S3 is about 440 and is found at pressure of 0.45 bar and nozzle position at about 24mm. In the opposite positioning of the nozzle we found the range of S3 is from 480 to 690. The minimum number of hairs S3 is found at pressure of 0.25 bar and position of 15 mm. Actually reduction of hairiness is about 30 % from the yarn produced without nozzle. This percentage is actually not satisfactory enough. This may be contributed to the spin tester,

finishing of the nozzles, and the lack of proper design of the nozzle, which is in the process of change.

3.4.6 Yarn Tenacity

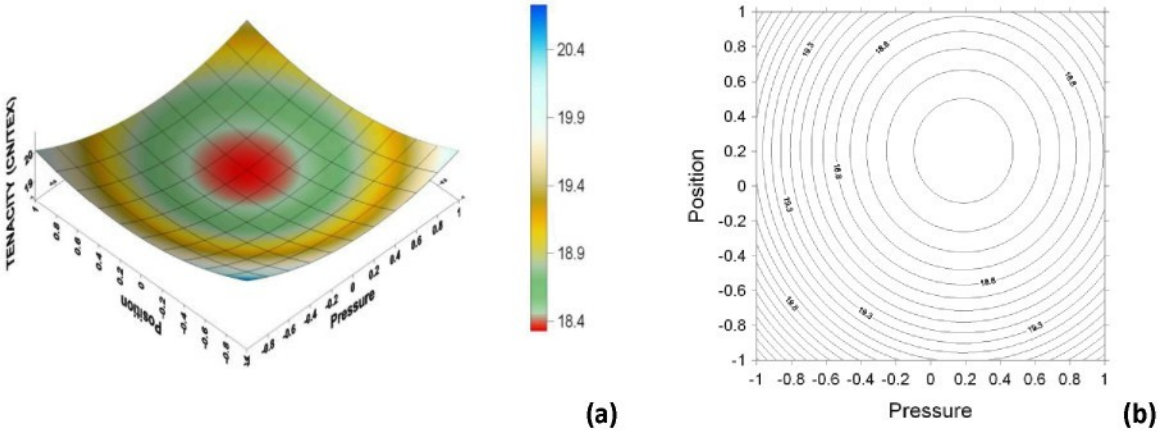

Fig. 37 Yarn Tenacity Vs. Position and Pressure (a) Response Surface (b) Contour Lines. Air Flow Downward.

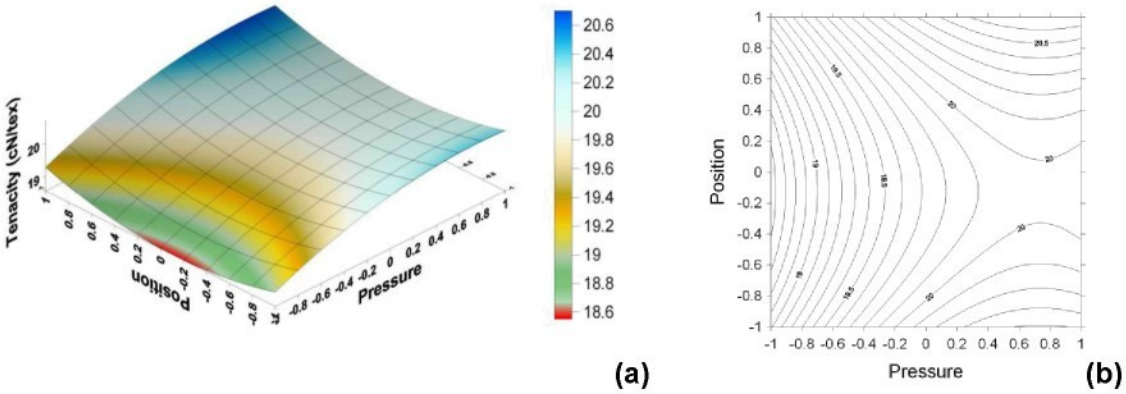

Fig. 38 Yarn Tenacity Vs. Position and Pressure (a) Response Surface (b) Contour Lines. Air Flow Upward.

It can be seen from figure 37 that, for downstream air flow, the yarn tenacity varies between 18.4 and 20.4 cN/Tex. The maximum tenacity is obtained either with maximum pressure and position or with the minimum pressure and position. In the opposite direction, as can be seen from fig 38, there is no significant change in minimum and maximum value of tenacity, but the maximum tenacity is obtained with maximum pressure of about 0.75 bar and a position of 33 mm from front roller nip.

3.5 Comparison between ring-jet trials and conventional ring yarn

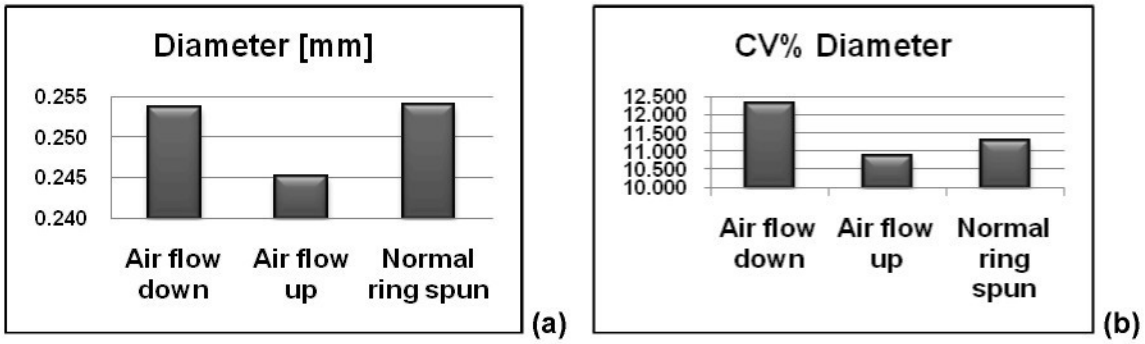

Fig. 39 Comparison ring-jet and normal yarn (a) Diameter (b) CV% Diameter

It can be seen from Figure 39 that the upward airflow resulted in a reduction of 10% in yarn diameter. The CV% diameter did not show a favourable comparison with normal yarn being 14% higher.

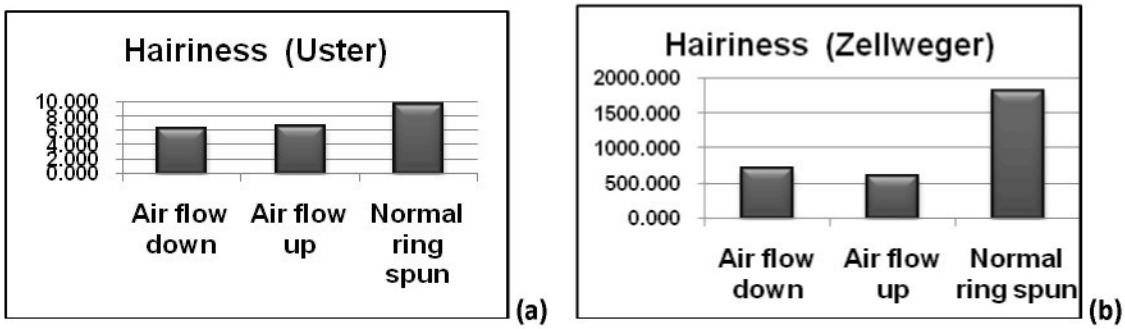

Fig. 40 Comparison ring-jet and normal yarn (a) CV% Mass (b) Uster Hairiness

The hairiness values obtained both from Uster and Zellweger showed significant improvement in hairiness values 35% and 65% respectively.

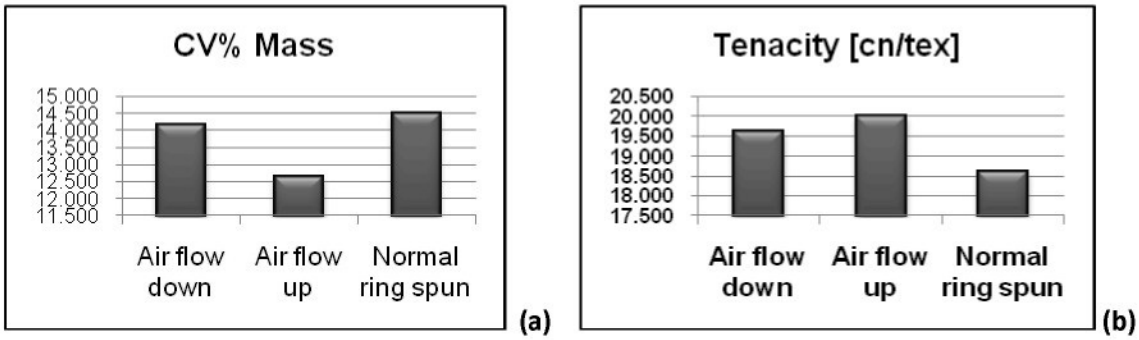

Fig. 41 Comparison ring-jet and normal yarn (a) Zellweger Hairiness (b) Tenacity

The CV% mass for airflow in the downward direction resulted in an improvement of 13%. The tenacity showed a marginal improvement of 5%.

4 Experimental Part -- Air-Jet

In relation to this part of the work it has to be emphasised at the onset that it is an attempt to produce yarns using only air-jets together with the ancillary fiber tube. The air-jets as well as other components have been manufactured in the local workshop. The drafting system of the conventional ringframe was used but the spindle eliminated and just the air jets were responsible for the insertion of twist. Material used was 100% cotton and 100% polyester. The yarn count spun was 28 tex using single roving and 56 tex using two rovings.

4.1 Components and attachment of the lower jet

The upper air-jet used was the same as in 3.4, and the components of the lower air-jet for the series arrangement is as depicted in Figure 42, and its mounting on the machine as shown in Figure 43. In comparison to the upper jet, the lower jet is larger with a protruding base since a higher pressure is used and it can accommodate the fiber feed ancillary tube.

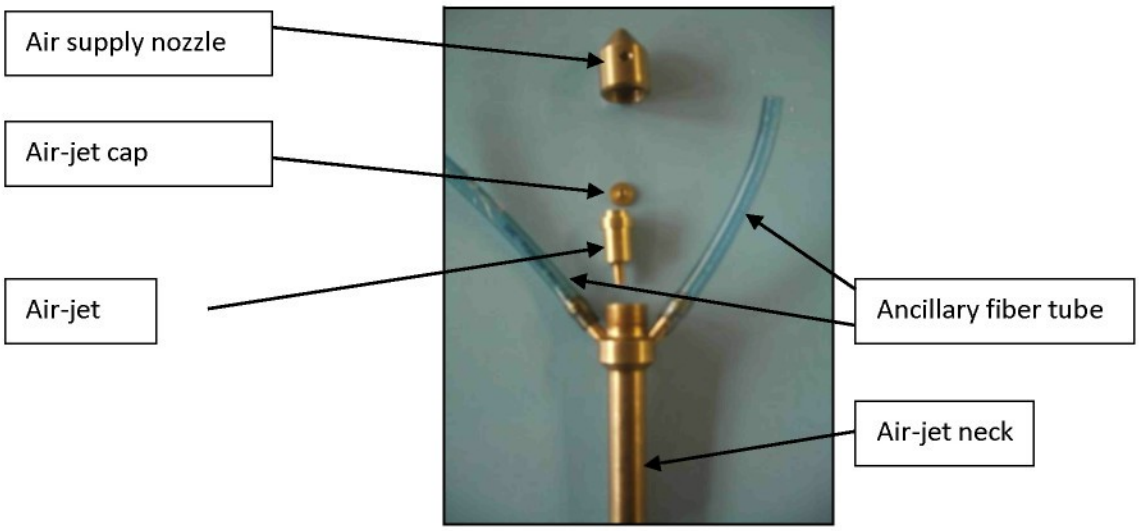

Fig. 42 Components of lower jet for series arrangement

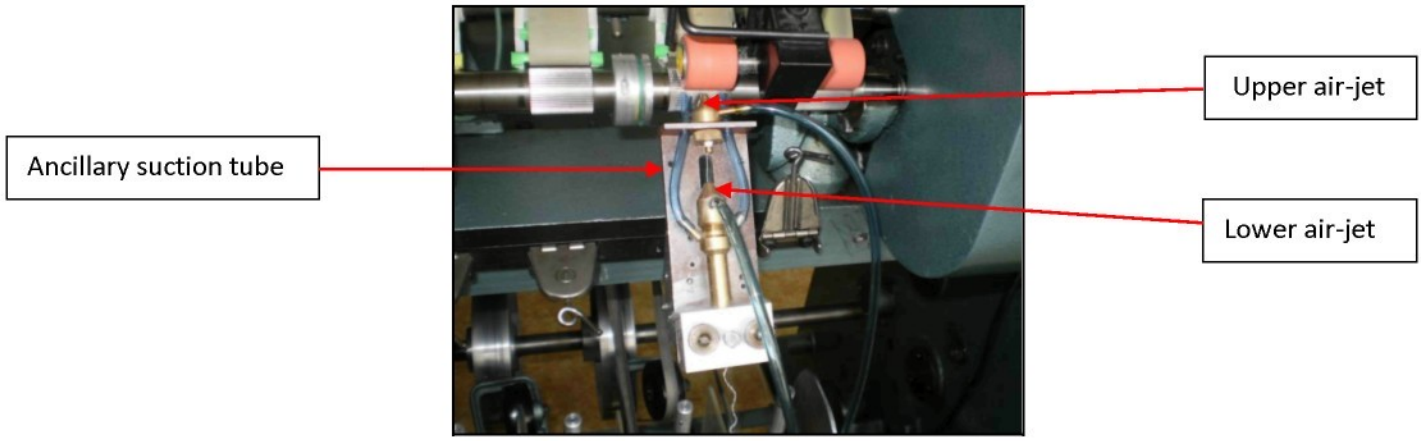

Fig. 43 Air-jets in Series

In an attempt to create a siro-spun effect, two jets were arranged in parallel and the third in series as shown in Figure 44.

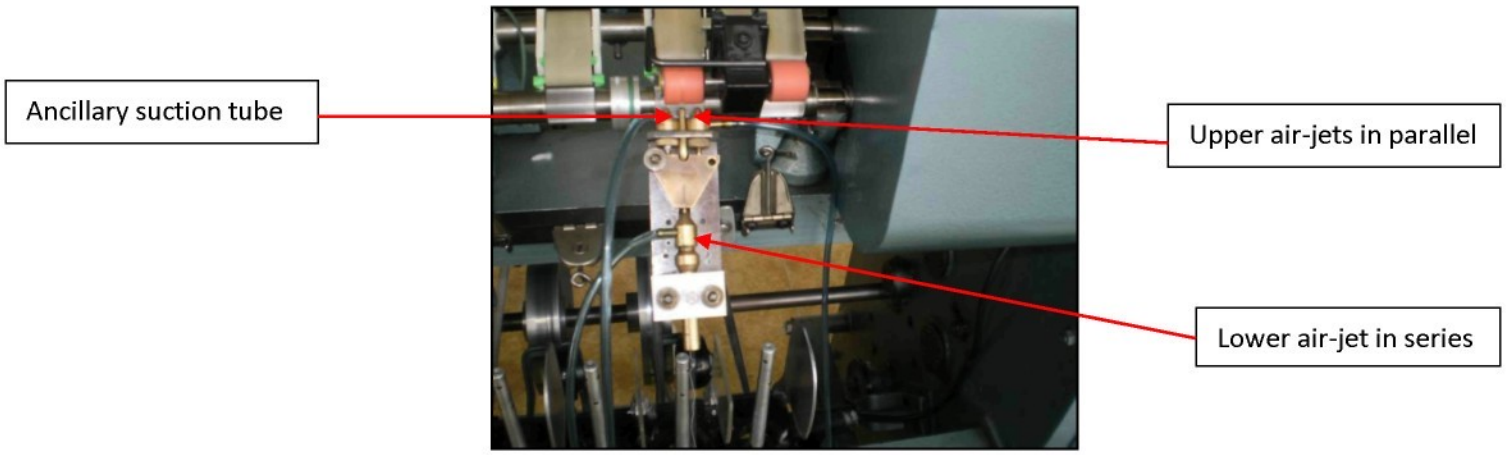

Fig. 44 Air-jets in series - parallel combination

4.2 Ancillary fiber tube

The concept of the ancillary fiber tube is to suck edge fibers at the delivery, thereby reducing their chances of them resulting in hairs, and feeding them to the second air-jet to incorporate them in the yarn structure as wrapper or belt fibers. It is assumed that the distribution of these fibers is three dimensional as in air vortex spinning. This effect would be enhanced with in the case of where two such tubes are attached to either side of

the lower jet as shown in Figure 26. Due to construction and design constraints, one such tube was used for air-jets in the series parallel combination.

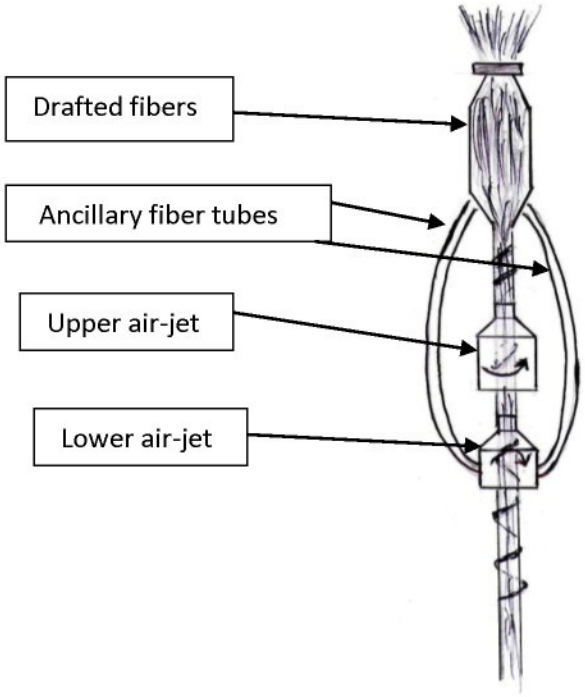

Fig. 45 Ancillary fiber tube

4.3 Winding mechanisms used

The following two winding mechanisms were utilized, the first as shown in Figure 46(a) was manufacture in the local workshop and the other a single winding head as shown in Figure 26(b). In both instances the speed was regulated by frequency, using the regulator as depicted in Figure 47(c).

(a)

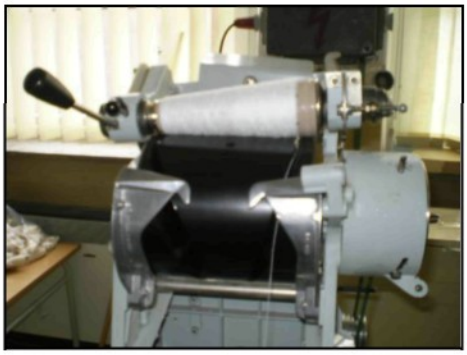

(b)

Fig. 46 Winding heads

(a)

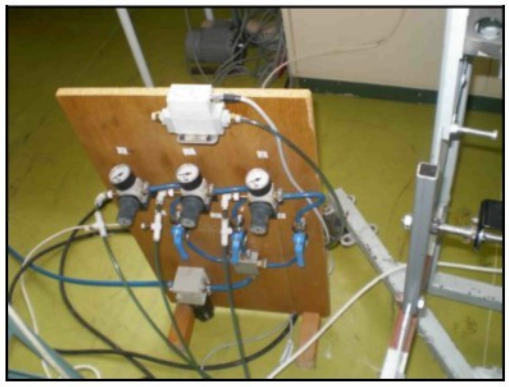

(b)

Fig. 47 Frequency regulator (a) and pressure regulator (b)

4.4 Results and Discussion

No physical tests could be conducted on the yarns that were produced using only the air jets. This was due to the yarn lacking sufficient uniformity of strength. The major reason for this is that the yarn, upon withdrawal from the jet lacked sufficient or rather was withdrawn with variation in tension which was the consequence of the poor winding device that was utilised. The fiber duration in the jet therefore varied, and in certain instances, was withdrawn too quickly, resulting in weak places. In the opposite case when take-off is slow, a kinked structure results. See Figure 48.

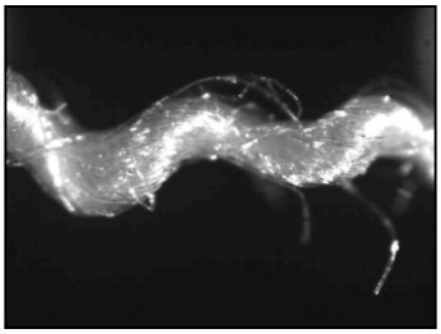

Fig. 48 Kinked yarn structure

With proper take-off and winding conditions, the desired effect was achieved by the air-jet together with the ancillary fiber feed tube. The photograph shown below in Figure 49 depicts the central core and the wrapper fibers around the periphery of the yarn. For portions of yarn that could be tested tenacity values of as high as 22 cN/tex were obtained.

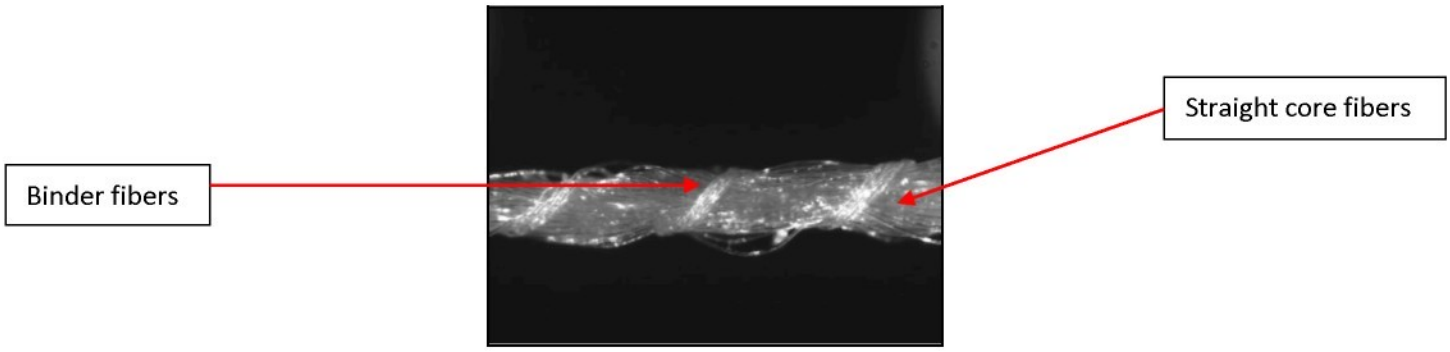

Fig. 49 Photomicrograph showing binder fibers

A problem with fiber accumulation with time in the ancillary tubes was also encountered. This was as a result of welding edges on the inside not being totally smoothened out as well as the angle of attachment of the tube. The other was the problem with static associated with the use of plastic tubes.

5. Conclusion

The yarns produced on the ring-jet system showed marked improvement in CV% mass and yarn tenacity and a drastic improvement in yarn hairiness measured both on the Uster and Zweigle systems and was especially pronounced with air flow in the upward direction. This was in keeping with theoretical expectations.

In the case of upward airflow, the air-jet induces an upward swirling air flow against yarn movement therefore most of the protruding fiber ends correspond to fiber tails for ring spun yarns. Therefore the air flow in the direction of yarn movement promoted, rather than suppressed these protruding fiber ends. Furthermore, since the swirling air current in the jet, twists the yarn strand in the reverse direction, the twist level in the strand above the jet is lower than that in the strand below the jet. Therefore, as the fiber strand traverses through the jet, the structure first gets loosened to some extent and then tightens up again as it emerges from the jet. This loosening and tightening up of the strand structure facilitates in tucking of the fiber ends into the body of the yarn, thus effectively reducing the hairiness.

For air-jet spun yarns, no physical tests could be conducted because of the inconsistency in the strength. The photomicrographs however reveal the presence of wrapper fibers binding the yarn core. This strength inconsistency was attributed to tension variations after the yarn emerged from the air-jet. For the yarn portions that could be tested for strength, the tenacity compared favourabally to equivalent ring spun yarn.

The structure of the yarn in the photomicrograph clearly depicts a central core of nearly parallel fibers with the wrapper fibers binding them together in a yarn. The distribution of the wrapper fibers, in a three dimensional manner rather than a two dimensional manner as is in conventional air- jet spinning, relates closely to that of vortex yarn produced by Murata. This is as a result of the ancillary fiber feed tube, re-channeling fibers from the delivery at the front roller to the second jet, promoting the creation of the wrapper or binder fibers.

The project was conducted entirely under laboratory conditions, meaning that the yarn was spun on a modified ringframe and components of the air-jet fabricated by the

workshop. These posed several constraints and listed below and are the major factors accountable for difficulty in producing yarn on the air –jet system.

- Spinning machinery old.
- Jet components fabricated in the workshop from brass – lacked desired accuracy and reproducibility.
- Inconsistent winding tension due to low winding speeds and improper winding equipment.

Future recommendations are as listed below:

- Simulate air current in the air-jet to obtain correct dimensions such as size, inclination and direction of holes.
- Use of plexiglass or transparent material for the jet housing to view the motion of the fibers within the jet.
- Use of tracer fibers to determine fiber motion and assembly within yarn structure.
- Attachment of a take-off roller at the exit of the jet and synchronise the speed to provide uniform tension.
- Use of sliver as feed material with an appropriate drafting arrangement.
- Use of a material with very smooth surface for the ancillary tube.

6. References

1. Artzt, P., "Short-Staple-Spinning-Surprises Confined to Detail" *Inemational Texile. Buletin.* Yarn Fabric Forming, 41, (4th Quarter,1995): 8-10.
2. Artzt, P., "Yarn Structures in Vortex Spinning" *Melliand International,* 6, June 2000: 107.
3. Barella, A., "The Hairiness of Yarns." *Textile Progress*, 13(1), 1983.
4. Basu, A., "Progress in Air-jet Spinning." *Textile Progress,* 29(3) 1999.
5. Cheng, K.P.S., Li, C.H.L., "JetRing Spinning and Its Influence on Yarn Hairiness." *Textile Research Journal.* 72(12), 2002:1079-1087.
6. Gray, W. M., "How MVS Makes Yarns." *12th Annual Engineer Fiber Selection System Conference Papers,* May 17 -19, 1999.
7. Gray, W. A., "An Update on Air-jet Spinning." *Textile Tecnology. International,* 25, 1993: 105-109.
8. Goswami, B. C., "New Technology Challenges Conventional Spinning Systems." *ATI,* 27, December 1998: 69-70.
9. Goswami, B. C., Martindale, J. G., and Scardino, E L., *Textile Yarns: Technology, Structure and Applications,* John Wiley & Sons, New York, 1997.
10. Heuberger, O., Ibrahim, S. M., and Field, N.C., "The Technology of Fasciated Yarns." *Textile Research. Journal.,* 41, 1971: 768-773.
11. Kalyanaraman, A.R., "A process to control hairiness in yarn." *Journal of the Textile Institute*., 83(3), 1992:407-413.
12. Krause, H. W., and Soliman, H.A., "Theoretical study of wrapping Twist in Single Jet False Twist Spinning." *Textile Research. Journal*., 59(9), 1989: 546-552.
13. Klein, W., *New Spinning Systems*. The Textile Institute Manual of Textile Technology, Stephen Austin and Sons Limited, UK, 1993.
14. Klein, W., *The Technology of Short-staple Spinning*. The Textile Institute Manual of Textile Technology, Alden Press, Oxford, UK, 1887.
15. Lawrence, C.A., *Fundementals of Spun Yarn Technology,* CRC Press, Florida, 2003.
16. McCreight, D. J., Feil, R. W., Booterbaugh, J. H., and Backe, E. E., *Short Staple Yarn Manufacturing*, 1997, Carolina Academic Press. Durham, NC USA.

17. Meyer, U., "Compact Yarns: Innovation as a Sector Driving Force." *Melliand International,* 6, March 2000: 2.
18. Montgomery, D.C., *Design and analysis of experiments*. 5th ed. New York: John Wiley, 2001.
19. Murata Machinery Limited, No. 851 Murata Vortex Spinner, Customer Information Brochure.
20. Nakahara, T., "Air-jet Spinning Technology." *Texile Technology International.,* 1988: 73-74.
21. Oxtoby, E., *Spun Yarn Technology,* Butterworth-Heinemann, Woburn, MA, 1987.
22. K P R Pillay., "A Study of The Hairiness of Cotton Yarns, Part I : Effect of Fiber and Yarn Factors." *Journal of Textile Research*, 34, 1994: 663-674.
23. Ramachandralu, K., Dasaradan, B.S. 2003., „Design and Fabrication of Air Jet Nozzles for Air Vortex Ring Spinning System to reduce Hairiness of Yarn." *Textile Research Journal,* 84, 2003: 6-9.
24. Rieter K45 ComforSpin Machine Brocure 2163 – v1.
25. Suessen Spinnovation No. 17.
26. Toray Engineering Ltd., "Toray AJS: 101- An Economic Air-jet Spinning Technology." *Textile World,* 136, (April 1986): 56-60.
27. Wang, X., Miao, M., and How,Y.L., "Studies of Jet Ring Spinning, Part I :Reducing Yarn Hairiness with the Jet Ring." *Journal of Textile Research*, 6(4), 1997: 253-258.
28. Witczak, D., GOLANSKI, J., "Airflow in the air-jet false twisting chamber." *Fibers and Textiles in Eastern Europe* July / September 2007, 15(3).
29. Zeng, Y.C., and Yu, C.W., "Numerical and Experimental Study on Reducing Yarn Hairiness with Jetring and Jetwind." *Textile Research Journal,* 74(3), March 2004: 222-223.
30. Zeng, Y.C., Wang, K.F., and Yu C.W. 2004. "Predicting the Tensile Properties of Air-Jet Spun Yarns." *Textile Research Journal.* 74(8), 2004: 689-694.
31. Zinser CompACT^3 – Short Staple Brocure.

Appendix

Table 1 Test results for ring-jet using downward airflow

Sample	Pressure Level	Position	Holes	Dia. (mm)	CV Di. (%)	CV% Mass	Hair (Uster)	Hair (Zweigle))	Tenacity (cN/Tex)
T1	-1	-1	0	0.253	11.52	13.16	5.88	742	20.822
T2	-1	1	0	0.25	11.76	13.53	5.83	740	19.779
T3	1	1	0	0.27	13.4	14.28	7.48	1136	19.64
T4	1	-1	0	0.261	12.2	13.58	6.65	939	20.045
T5	0	1	1	0.256	12.93	14.74	6.22	918	19.474
T6	0	-1	1	0.256	12.24	14.2	6.18	805	19.574
T7	0	-1	-1	0.248	11.77	14.02	5.65	771	19.915
T8	0	1	-1	0.256	12.26	14.33	6.09	760	18.86
T9	1	0	1	0.252	12.4	14.41	6.2	458	19.703
T10	1	0	-1	0.252	12.61	14.78	6.26	421	18.507
T11	-1	0	1	0.247	12.16	14.26	5.91	457	19.657
T12	-1	0	-1	0.246	12.15	14.23	5.89	605	20.301
T13	0	0	0	0.251	12.31	14.31	6.03	443	18.393

Table 2 Test results for ring-jet using upward airflow

Sample	Pressure Level	Position	Holes	Dia. (mm)	CV Di. (%)	CV% Mass	Hair (Uster)	Hair (Zweigle))	Tenacity (cN/Tex)
AT1	-1	-1	0	0.242	10.87	12.51	6.64	573	18.84
AT2	-1	1	0	0.245	10.99	12.41	6.66	587	18.911
AT3	1	1	0	0.246	11.02	12.44	6.69	361	20.992
AT4	1	-1	0	0.243	11.27	12.75	6.77	593	20.862
AT5	0	1	1	0.246	10.81	12.3	6.43	695	20.728
AT6	0	-1	1	0.246	11.22	12.66	6.74	845	20.513
AT7	0	-1	-1	0.246	11.17	12.81	6.35	411	19.611
AT8	0	1	-1	0.246	11.11	12.62	6.55	674	20.342
AT9	1	0	1	0.246	10.78	12.5	6.25	749	20.106
AT10	1	0	-1	0.243	11.02	12.45	6.49	543	19.143
AT11	-1	0	1	0.247	10.93	12.09	6.26	742	19.538
AT12	-1	0	-1	0.247	10.97	12.64	6.34	412	18.237
AT13	0	0	0	0.245	10.7	12.19	6.39	672	19.909

Table 3 Comparitive test results between ring-jet and normal yarns

	Dia. (mm)	CV% Diam (%)	CV% Mass (%)	Hair (U)	Hair (Z)	Tenacity (cN/Tex)
Downward flow	0.254	12.285	14.141	6.175	707.308	19.590
Upward flow	0.245	10.841	12.630	6.418	586.615	19.992
Normal ring spun	0.284	11.27	14.5	9.5	1800	18.6